Supplementary Information for

Hermes et al: Thioesterase-mediated Side Chain Transesterification Generates Potent Gq Signaling Inhibitor FR900359, *Nat. Comm.* **2020**

Content

Characterization of *C. vaccinii* as FR Producer

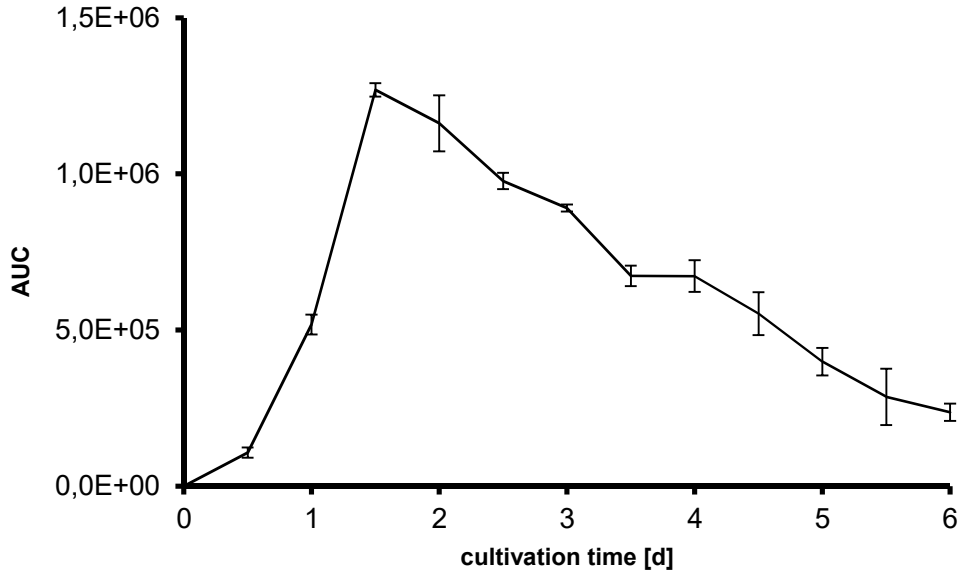

Supplementary Figure 1: FR production in *C. vaccinii*. Production curve for FR (**1**) from *C. vaccinii* cultivation in LB. Area under the curve of extracted *m/z:* 1002.54 is plotted. Data are presented as mean values ± SD. Experiments were performed in triplicate.

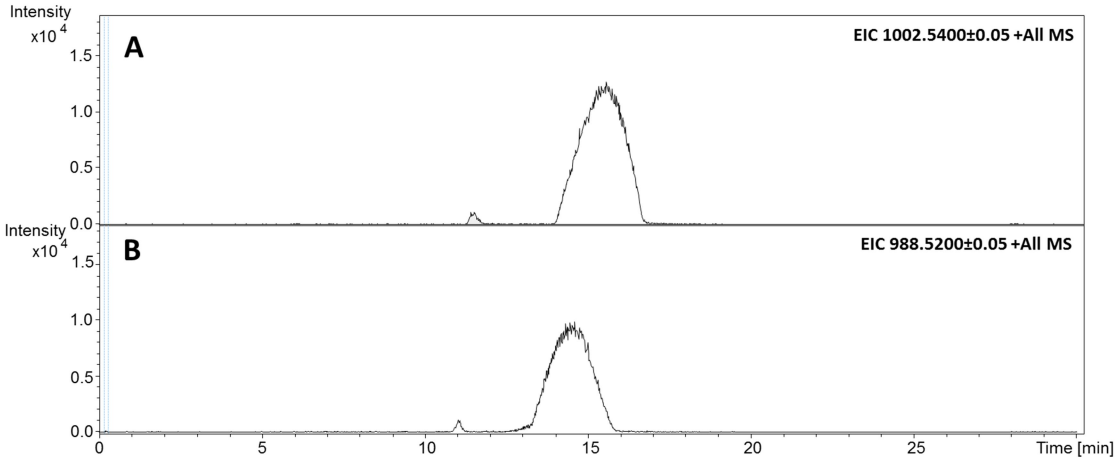

Supplementary Figure 2: FR and FR-2 comparison. Extracted ion chromatograms (EIC) of FR (**1**, *m/z*: 1002.54 ± 0.05, A) and FR-2 (**3**, *m/z*: 988.52 ± 0.05, B) from *C. vaccinii n*-butanol extracts. Cultures were grown in LB medium for 36 h.

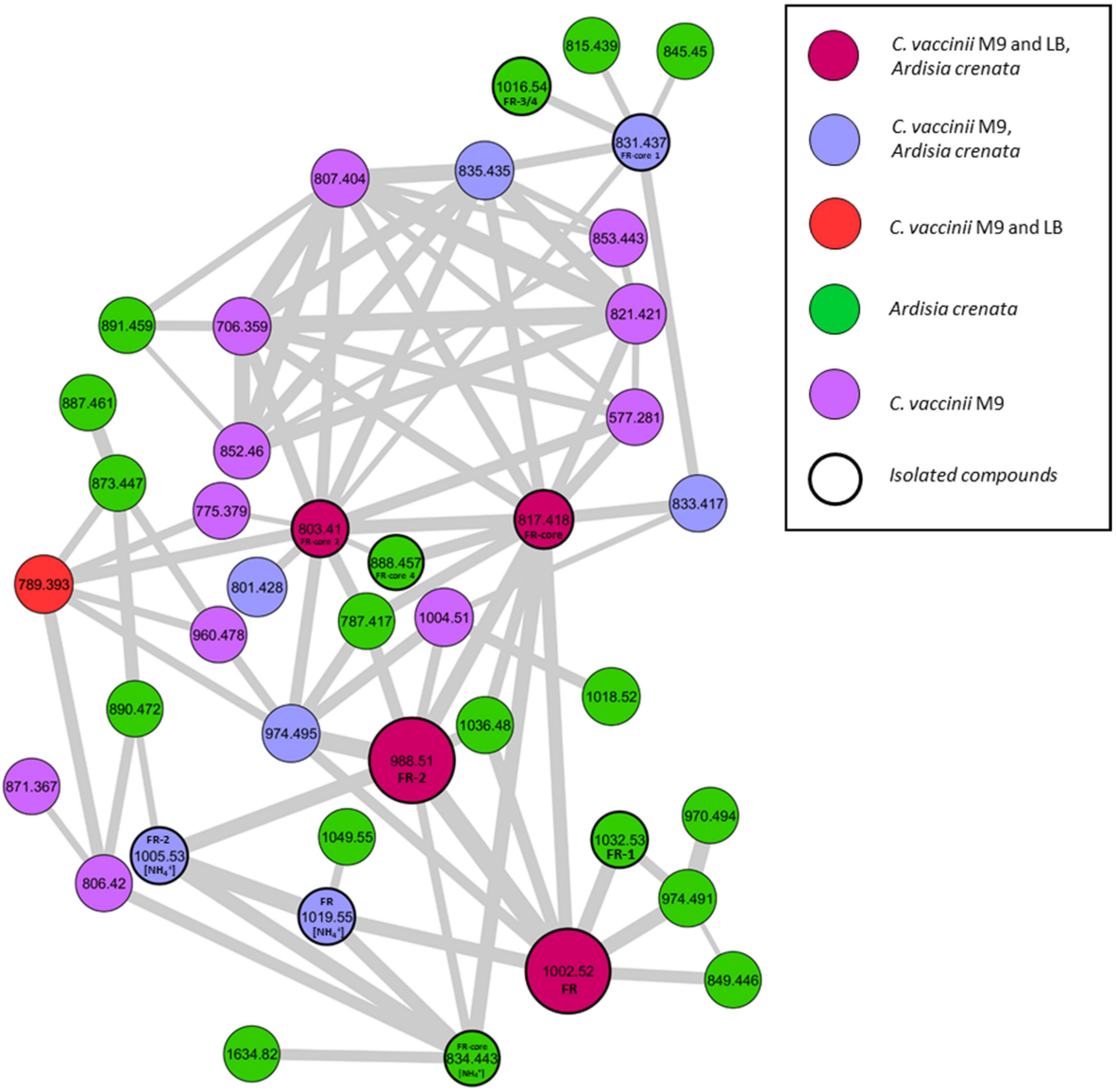

Supplementary Figure 3: Molecular network of FR and its derivatives from different producers: *C. vaccinii* in M9 and LB medium and "*Ca.* B. crenata" in *A. crenata*. Nodes display distinct *m/z* features, representing their parent mass and their size represents the number of spectra found. The width of the edges represents the similarity of the fragmentation spectra of the two masses, while the color of the node displays the origin of production (magenta: all extracts; purple: only produced by *C. vaccinii* in M9 medium; green: only produced by *Ca.* B. crenata; red: produced by *C. vaccinii* in LB and M9 medium; blue: produced by "*Ca.* B. crenata" and *C. vaccinii* in M9 medium). Derivatives already known and published are indicated in the respective nodes.

Gap Closure and Bioinformatic Analysis of *C. vaccinii frs*

Gap closure of *C. vaccinii frs* BGC

To analyze the genome of *C. vaccinii* MWU205, genomic DNA was prepared from a freshly grown overnight culture with the GenElute Bacterial Genomic DNA Kit (Merck) and sent to Göttingen Genomics Laboratory (G2L, Göttingen) for Illumina sequencing. The resulting draft genome (4.998 Mb in 79 contigs) was then applied to homology guided alignments using the Geneious Pro 5.6.7 software (Biomatters Ltd.), which yielded eight contigs (42, 43, 46, 47, 50, 61, 62, 63) harboring parts of a potential FR gene cluster. When mapped to the *frs* gene cluster of "*Ca*. B. crenata",[1] a potential position for six of them (42, 43, 46, 47, 50, 63) could be determined (Supplementary Fig. 4). For the remaining two contigs, no clear mapping was possible, as they covered reoccurring regions within the *frs* gene cluster (61: A domain identity, 62: MT domain identity). This contig assignment suggested the presence of five gaps. To close these, specific primers binding 130-450 bp upstream of the contig ends were designed (Supplementary Table 1) and applied for PCR-based gap closure. All PCR reactions (25 µL scale) consisted of: 1x Q5 reaction buffer, 1x Q5 GC enhancer, 200 µM dNTPs, 500 nM of forward and reverse primer, 2.25 ng of *C. vaccinii* gDNA and 0.01 U/µL Q5 High-Fidelity DNA polymerase (NEB). Thermal cycling was performed in a Biometra TGradient cycler with an initial denaturation step at 98 °C for 30 s, followed by 30 to 33 cycles of DNA denaturation at 98 °C for 10 s, primer annealing for 20 s and DNA amplification at 72 °C for 30 s/kb amplified, and a final extension step at 72 °C for 2 min. Optimal annealing temperature for specific primer combinations was determined experimentally using temperature gradients from 46–64 °C. PCR products of the expected size were purified and subsequently submitted to terminal-end Sanger sequencing along with the primers used for amplification. Where necessary, primer walking was applied for the sequencing of larger PCR products (see primers in Supplementary Table 1).

Supplementary Table 1: Primers used in this study. Restriction sites are bold, Gibson homology arms are underlined. All overhangs are given in lowercase, while target specific sequences are given in uppercase. Restriction sites are bold.

Name	Sequence (5' → 3')	Description
BamHI-FRT_for	tga **ggatcc** AGCTTCAAAAGCGCTCTGA	Sequential cloning of FRT into pUC19
SalI-FRT_rev	tgt **gtcgac** GGGGATCTTGAAGTTCCT	Sequential cloning of FRT into pUC19
SphI-frsA-up_for	agt **gcatgc** GGAAAGTACGTCTGGTCTTG	Sequential cloning of the *frsA*-up region into pUC19::FRT
SalI-frsA-up_rev	tct **gtcgac** TACATCCAGCTGTGCTGAAG	Sequential cloning of the *frsA*-up region into pUC19::FRT
BamHI-frsA-dn_for	ttc **ggatcc** ATTGGTCCTGTTCTCGAGTC	Sequential cloning of the *frsA*-dn region into pUC19::*frsA*-up-FRT
SacI-frsA-dn_rev	tga **gagctc** AGTCCCGCATATGATCGATG	Sequential cloning of the *frsA*-dn region into pUC19::*frsA*-up-FRT
FRT_for	CGAATTAGCTTCAAAAGCGCTCTGA	One step cloning of FRT into pEX18Tc
FRT_rev	CGAATTGGGGATCTTGAAGTTCCT	One step cloning of FRT into pEX18Tc
Gib-vioA-up_for	gcatgcctgcaggtcgactctaga**g gatcc** TGACCCTTGGAACAGGATG	One step cloning of *vioA*-up into pEX18Tc
FRT-vioA-up_rev	aggaacttcaagatccccaattcg CTGCTGCATGTCGAAAATG	One step cloning of *vioA*-up into pEX18Tc
FRT-vioA-dn_for	tcagagcgcttttgaagctaattcg CGTCCATGTGCACAAGTAC	One step cloning of *vioA*-dn into pEX18Tc
Gib-vioA-dn_rev	tacgaattcgagctcggtacccggg GCTCGCCATTGATCGAAAC	One step cloning of *vioA*-dn into pEX18Tc
PCR-frsA-KO_for	GTAATGTCAAAGGCTTGG	Mutant verification of *C. vaccinii* Δ*frsA* by PCR / Sequencing
PCR-frsA-KO_rev	ATTGAATTGCTGACACCG	Mutant verification of *C. vaccinii* Δ*frsA* by PCR / Sequencing
PCR-vioA-KO_for	AGCTCTACCTGTGGCAG	Mutant verification of *C. vaccinii* Δ*vioA* by PCR / Sequencing
PCR-vioA-KO_rev	TCCCAGGAGAAATGGTTG	Mutant verification of *C. vaccinii* Δ*vioA* by PCR / Sequencing
Gap1_for	TCGAGATGATGAAGGCTG	PCR-based closure of gap 1/ Sequencing
Gap1_rev	GGCATCAACACTTGATAAG	PCR-based closure of gap 1/ Sequencing
Gap2_for	TCCACCTCGATTTGTACG	PCR-based closure of gap 2 / Sequencing
Gap2_rev	CATGATCAACTCCTGACAG	PCR-based closure of gap 2 / Sequencing
Gap3_for	ATCTGGAACACCCGAATC	PCR-based closure of gap 3 / Sequencing
Gap3_rev	CAACTGGGCAACATAGCTG	PCR-based closure of gap 3 / Sequencing
Gap4_for	CGACTTGTTCTTCAATCTG	PCR-based closure of gap 4 / Sequencing
Gap4_rev	TCGAAACGATACAGGAACC	PCR-based closure of gap 4 / Sequencing
Gap5_for	CCCAATCATCTGGTATTGC	PCR-based closure of gap 5 / Sequencing
Gap5_rev	CCCAATCATCTGGTATTGC	PCR-based closure of gap 5 / Sequencing
Gap1_rev2	CATCCAGCACGTACAGC	Sequencing / Primer walking
Gap1_rev3	AGGCTTTGCAGATGGCG	Sequencing / Primer walking
Gap2_for2	CCTATGTGATCTACACCTC	Sequencing / Primer walking
Gap3_for2	TGCTGGAAATCGGCGTC	Sequencing / Primer walking
Gap4_for2	GGGTGACGCTGAATACG	Sequencing / Primer walking
Gap4_for3	AATACCCAGACCTACGTG	Sequencing / Primer walking
Gap4_rev2	CGAAGAAGCTGTCGTCC	Sequencing / Primer walking
Gap4_rev3	CCAGCAGCAGTTCCTTC	Sequencing / Primer walking
Cv_frsA-His6-N_for_BamHI	gat**ggatcc**ATGAAAAACAGTGAATCGC	In vitro studies
Cv_frsA-His6-N_rev_HindIII	tat**aagctt**TTATTGCTTGACAGCGGTGAC	In vitro studies
Cv-frsA-PCP-His6-N_rev_HindIII	tat**aagctt**tcaGCTGTCGCCGCCTTCGGC	In vitro studies
Cv-frsA-A-His6-N_for_BamHI	tat**ggatcc**CCGTCGCAGCCGGTGTCC	In vitro studies
Cv-frsA-TE-His6-N_for_BamHI	tat**ggatcc**GCCGAAGGCGGCGACAGC	In vitro studies
Cv_frsB_for_NdeI	gcg**catATG**AGCAATCCCTTTGATGAT	In vitro studies
Cv_frsB_rev_PacI_pCDF	gcg**ttaattaa**ttaTTTATCATCGCACTCCAT	In vitro studies
Cv_frsD-His6-N_for_HindIII	cac**aagctt**tgATGGAAATATGGCTGGCG	In vitro studies
Cv_frsD-His6-N_rev_XhoI	tat**ctcgag**TCAACTCCTGACAGCGTG	In vitro studies
Cv_frsH-His6-N_for_BamHI	gat**ggatcc**ATGACCGTATCCGATAAC	In vitro studies
Cv_frsH-His6-N_rev_XhoI	gata**ctcgag**tTACAGCAGCATGGTTTG	In vitro studies

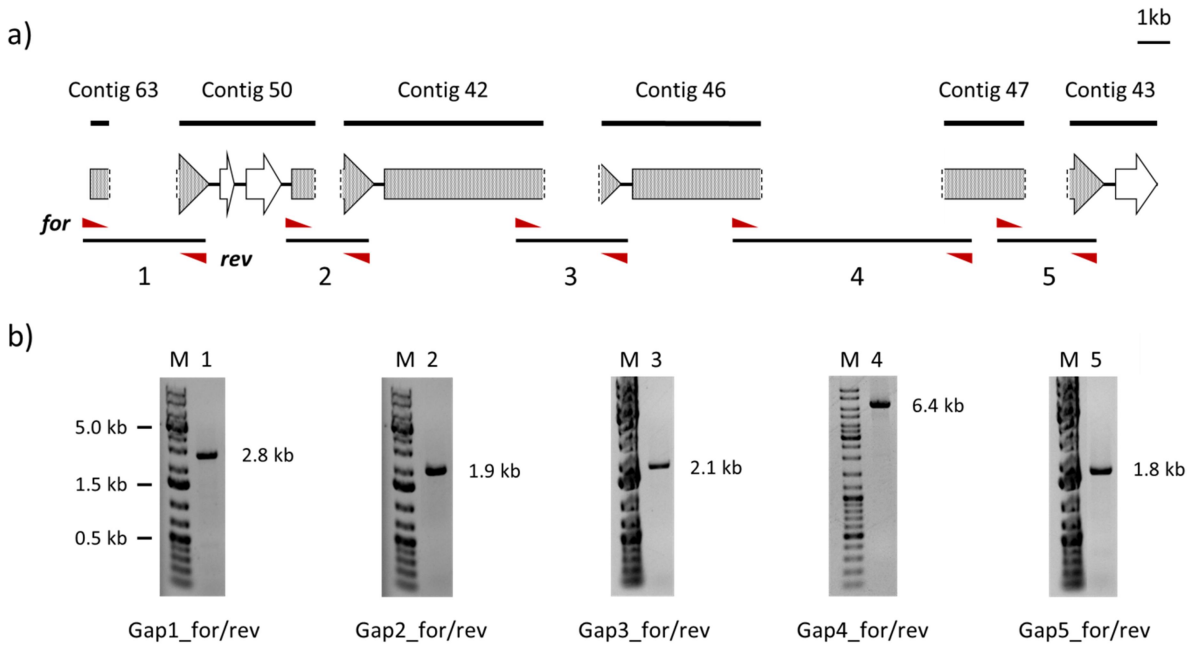

Supplementary Figure 4: Gap closure of the *C. vaccinii frs* BGC. a) PCR-based approach for closing the five potential gaps (1-5) within the gene cluster. Organization of the six contigs with *frs* identity shown here is based on the *frs* gene cluster from "*Ca.* B. crenata". Two additional contigs with *frs* identity (not shown) couldn't be assigned to a specific position. Binding sites of the respective forward (for) and reverse (rev) primers for each gap are indicated (red triangles). b) Q5-PCRs with the five primer pairs designed for gap closure (Gap1_for/rev to Gap5_for/rev). These experiments were independently repeated at least two times with similar results.

Supplementary Table 2: Annotation of *C. vaccinii* Frs proteins and closest homologues in the NCBI database (apart from "*Ca.* B. crenata" Frs proteins), revealed by BLAST searches.

Protein	Functional annotation	Closest homologue (NCBI Accession number)	Similarity/Identity (%/%)
FrsA	Nonribosomal Peptide Synthetase (C-A-T-TE)	WP_048411362. Non-ribosomal peptide synthase [Chromobacterium sp. LK1]	57/41
FrsB	MbtH-like protein	MBC7269998.1 MbtH family protein [Streptomyces sp.]	88/69
FrsC	Phenylpyruvate reductase	NCT40463. malate dehydrogenase [Alpha-proteobacteria bacterium]	65/53
FrsD	Nonribosomal Peptide Synthetase (C-A-T)	WP_184971800.1 amino acid adenylation domain-containing protein [Streptomyces echinatus]	59/46
FrsE	Nonribosomal Peptide Synthetase (C-A-T-E-C-A-MT-T)	WP_162791553.1 non-ribosomal peptide synthase/polyketide synthase [Dyella sp. L4-6]	63/52
FrsF	Nonribosomal Peptide Synthetase (C-A-T-C-A-MT-T)	WP_073766514.1 non-ribosomal peptide synthetase [Streptomyces sp. CB02923]	63/50
FrsG	Nonribosomal Peptide Synthetase (C-A-T-C-A-MT-MT-T-TE)	WP_162791553.1 non-ribosomal peptide synthase/polyketide synthase [Dyella sp. L4-6]	68/55
FrsH	Leucine-ß-hydroxylase	WP_168647361.1 MBL fold metallo-hydrolase [Dyella sp. SG609]	76/65

Supplementary Table 3: Comparison of genes and encoded proteins in the *frs* BGCs. Identities were calculated by using the EMBOSS needle alignment tool (EMBL-EBI).[2]

gene	*C. vaccinii* (nt)	"*Ca.* B crenata" (nt)	Identity nt (%)	*C. vaccinii* (aa)	"*Ca.* B crenata" (aa)	Identity aa (%)
frsA	3819	3768	70	1272	1255	71
frsB	219	219	72	72	72	75
frsC	987	987	68	328	328	72
frsD	3081	3078	70	1026	1025	70
frsE	9051	9048	70	3016	3015	71
frsF	7557	7560	73	2518	2519	75
frsG	9408	9411	72	3135	3136	73
frsH	1596	1599	77	531	532	85

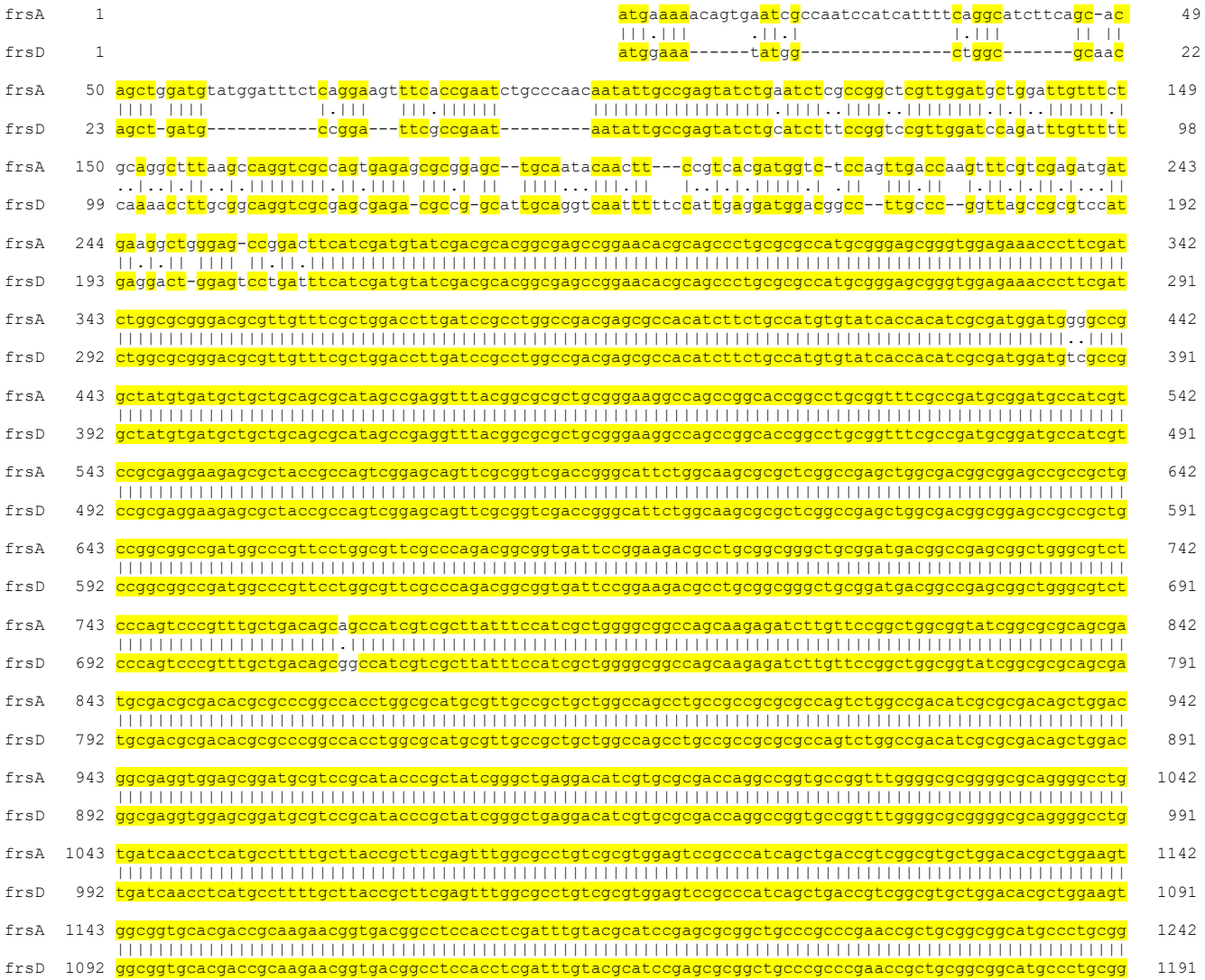

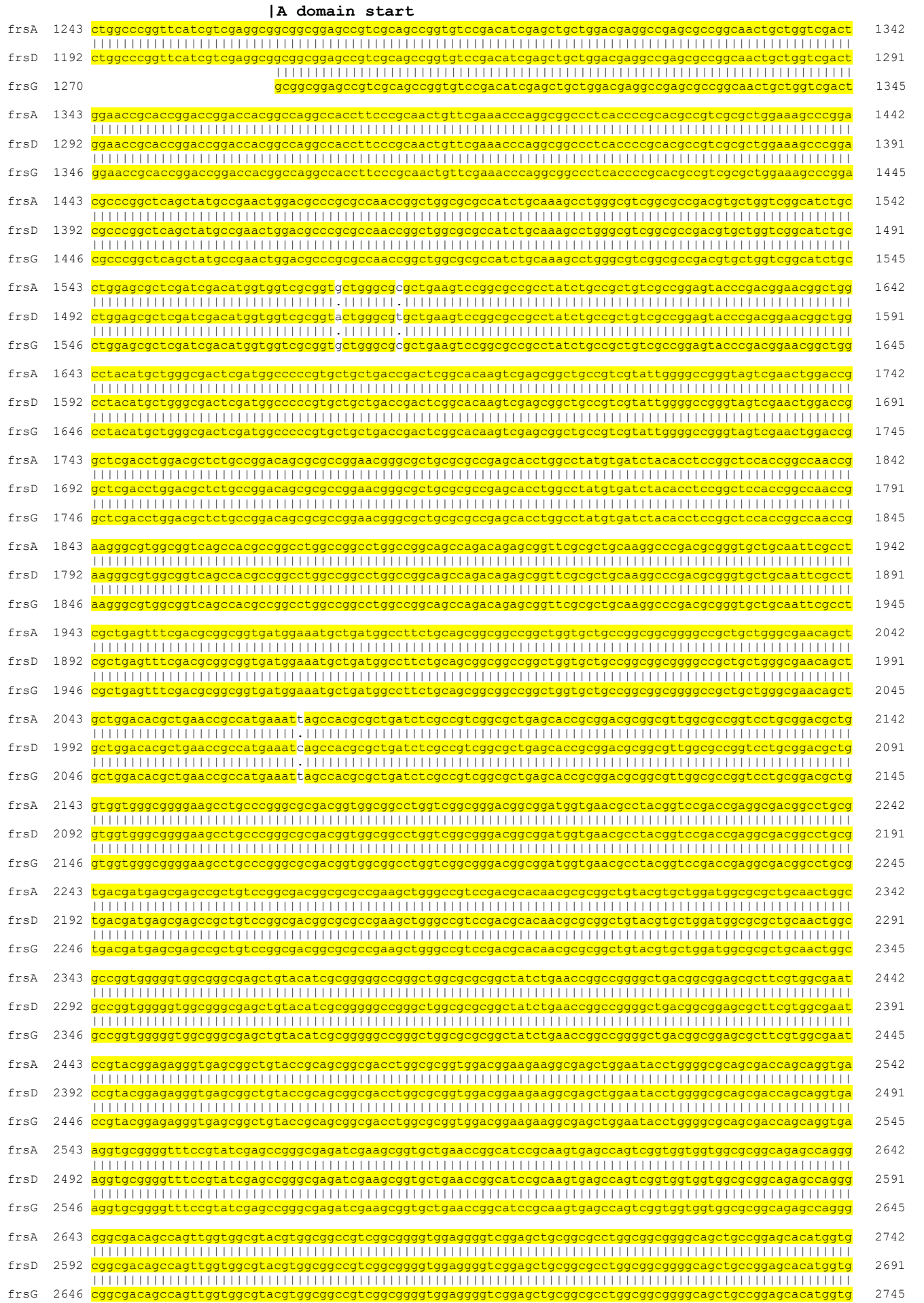
|A domain start
frsA 1243 ctggcccggttcatcgtcgaggcggcggcggagccgtcgcagccggtgtccgacatcgagctgctggacgaggccgagcgccggcaactgctggtcgact 1342
frsD 1192 ctggcccggttcatcgtcgaggcggcggcggagccgtcgcagccggtgtccgacatcgagctgctggacgaggccgagcgccggcaactgctggtcgact 1291
frsG 1270 gcggcggagccgtcgcagccggtgtccgacatcgagctgctggacgaggccgagcgccggcaactgctggtcgact 1345
frsA 1343 ggaaccgcaccggaccggaccacggccaggccaccttcccgcaactgttcgaaacccaggcggccctcaccccgcacgccgtcgcgctggaaagcccgga 1442
frsD 1292 ggaaccgcaccggaccggaccacggccaggccaccttcccgcaactgttcgaaacccaggcggccctcaccccgcacgccgtcgcgctggaaagcccgga 1391
frsG 1346 ggaaccgcaccggaccggaccacggccaggccaccttcccgcaactgttcgaaacccaggcggccctcaccccgcacgccgtcgcgctggaaagcccgga 1445
frsA 1443 cgcccggctcagctatgccgaactggacgcccgcgccaaccggctggcgcgccatctgcaaagcctgggcgtcggcgccgacgtgctggtcggcatctgc 1542
frsD 1392 cgcccggctcagctatgccgaactggacgcccgcgccaaccggctggcgcgccatctgcaaagcctgggcgtcggcgccgacgtgctggtcggcatctgc 1491
frsG 1446 cgcccggctcagctatgccgaactggacgcccgcgccaaccggctggcgcgccatctgcaaagcctgggcgtcggcgccgacgtgctggtcggcatctgc 1545
frsA 1543 ctggagcgctcgatcgacatggtggtcgcggtgctgggcgcgctgaagtccggcgccgcctatctgccgctgtcgccggagtacccgacggaacggctgg 1642
frsD 1492 ctggagcgctcgatcgacatggtggtcgcggtactgggcgtgctgaagtccggcgccgcctatctgccgctgtcgccggagtacccgacggaacggctgg 1591
frsG 1546 ctggagcgctcgatcgacatggtggtcgcggtgctgggcgcgctgaagtccggcgccgcctatctgccgctgtcgccggagtacccgacggaacggctgg 1645
frsA 1643 cctacatgctgggcgactcgatggcccccgtgctgctgaccgactcggcacaagtcgagcggctgccgtcgtattggggccgggtagtcgaactggaccg 1742
frsD 1592 cctacatgctgggcgactcgatggcccccgtgctgctgaccgactcggcacaagtcgagcggctgccgtcgtattggggccgggtagtcgaactggaccg 1691
frsG 1646 cctacatgctgggcgactcgatggcccccgtgctgctgaccgactcggcacaagtcgagcggctgccgtcgtattggggccgggtagtcgaactggaccg 1745
frsA 1743 gctcgacctggacgctctgccggacagcgcgccggaacgggcgctgcgcgccgagcacctggcctatgtgatctacacctccggctccaccggccaaccg 1842
frsD 1692 gctcgacctggacgctctgccggacagcgcgccggaacgggcgctgcgcgccgagcacctggcctatgtgatctacacctccggctccaccggccaaccg 1791
frsG 1746 gctcgacctggacgctctgccggacagcgcgccggaacgggcgctgcgcgccgagcacctggcctatgtgatctacacctccggctccaccggccaaccg 1845
frsA 1843 aagggcgtggcggtcagccacgccggcctggccggcctggccggcagccagacagagcggttcgcgctgcaaggcccgacgcgggtgctgcaattcgcct 1942
frsD 1792 aagggcgtggcggtcagccacgccggcctggccggcctggccggcagccagacagagcggttcgcgctgcaaggcccgacgcgggtgctgcaattcgcct 1891
frsG 1846 aagggcgtggcggtcagccacgccggcctggccggcctggccggcagccagacagagcggttcgcgctgcaaggcccgacgcgggtgctgcaattcgcct 1945
frsA 1943 cgctgagtttcgacgcggcggtgatggaaatgctgatggccttctgcagcggcggccggctggtgctgccggcggcggggccgctgctgggcgaacagct 2042
frsD 1892 cgctgagtttcgacgcggcggtgatggaaatgctgatggccttctgcagcggcggccggctggtgctgccggcggcggggccgctgctgggcgaacagct 1991
frsG 1946 cgctgagtttcgacgcggcggtgatggaaatgctgatggccttctgcagcggcggccggctggtgctgccggcggcggggccgctgctgggcgaacagct 2045
frsA 2043 gctggacacgctgaaccgccatgaaattagccacgcgctgatctcgccgtcggcgctgagcaccgcggacgcggcgttggcgccggtcctgcggacgctg 2142
frsD 1992 gctggacacgctgaaccgccatgaaatcagccacgcgctgatctcgccgtcggcgctgagcaccgcggacgcggcgttggcgccggtcctgcggacgctg 2091
frsG 2046 gctggacacgctgaaccgccatgaaattagccacgcgctgatctcgccgtcggcgctgagcaccgcggacgcggcgttggcgccggtcctgcggacgctg 2145
frsA 2143 gtggtgggcggggaagcctgcccgggcgcgacggtggcggcctggtcggcgggacggcggatggtgaacgcctacggtccgaccgaggcgacggcctgcg 2242
frsD 2092 gtggtgggcggggaagcctgcccgggcgcgacggtggcggcctggtcggcgggacggcggatggtgaacgcctacggtccgaccgaggcgacggcctgcg 2191
frsG 2146 gtggtgggcggggaagcctgcccgggcgcgacggtggcggcctggtcggcgggacggcggatggtgaacgcctacggtccgaccgaggcgacggcctgcg 2245
frsA 2243 tgacgatgagcgagccgctgtccggcgacggcgcgccgaagctgggccgtccgacgcacaacgcgcggctgtacgtgctggatggcgcgctgcaactggc 2342
frsD 2192 tgacgatgagcgagccgctgtccggcgacggcgcgccgaagctgggccgtccgacgcacaacgcgcggctgtacgtgctggatggcgcgctgcaactggc 2291
frsG 2246 tgacgatgagcgagccgctgtccggcgacggcgcgccgaagctgggccgtccgacgcacaacgcgcggctgtacgtgctggatggcgcgctgcaactggc 2345
frsA 2343 gccggtgggggtggcgggcgagctgtacatcgcgggggccgggctggcgcgcggctatctgaaccggccgggggctgacggcggagcgcttcgtggcgaat 2442
frsD 2292 gccggtgggggtggcgggcgagctgtacatcgcgggggccgggctggcgcgcggctatctgaaccggccgggggctgacggcggagcgcttcgtggcgaat 2391
frsG 2346 gccggtgggggtggcgggcgagctgtacatcgcgggggccgggctggcgcgcggctatctgaaccggccgggggctgacggcggagcgcttcgtggcgaat 2445
frsA 2443 ccgtacggagagggtgagcggctgtaccgcagcggcgacctggcgcggtggacggaagaaggcgagctggaatacctggggcgcagcgaccagcaggtga 2542
frsD 2392 ccgtacggagagggtgagcggctgtaccgcagcggcgacctggcgcggtggacggaagaaggcgagctggaatacctggggcgcagcgaccagcaggtga 2491
frsG 2446 ccgtacggagagggtgagcggctgtaccgcagcggcgacctggcgcggtggacggaagaaggcgagctggaatacctggggcgcagcgaccagcaggtga 2545
frsA 2543 aggtgcggggtttccgtatcgagccgggcgagatcgaagcggtgctgaaccggcatccgcaagtgagccagtcggtggtggtggcgcggcagagccaggg 2642
frsD 2492 aggtgcggggtttccgtatcgagccgggcgagatcgaagcggtgctgaaccggcatccgcaagtgagccagtcggtggtggtggcgcggcagagccaggg 2591
frsG 2546 aggtgcggggtttccgtatcgagccgggcgagatcgaagcggtgctgaaccggcatccgcaagtgagccagtcggtggtggtggcgcggcagagccaggg 2645
frsA 2643 cggcgacagccagttggtggcgtacgtggcggccgtcggcggggtggaggggtcggagctgcggcgcctggcggcggggcagctgccggagcacatggtg 2742
frsD 2592 cggcgacagccagttggtggcgtacgtggcggccgtcggcggggtggaggggtcggagctgcggcgcctggcggcggggcagctgccggagcacatggtg 2691
frsG 2646 cggcgacagccagttggtggcgtacgtggcggccgtcggcggggtggaggggtcggagctgcggcgcctggcggcggggcagctgccggagcacatggtg 2745

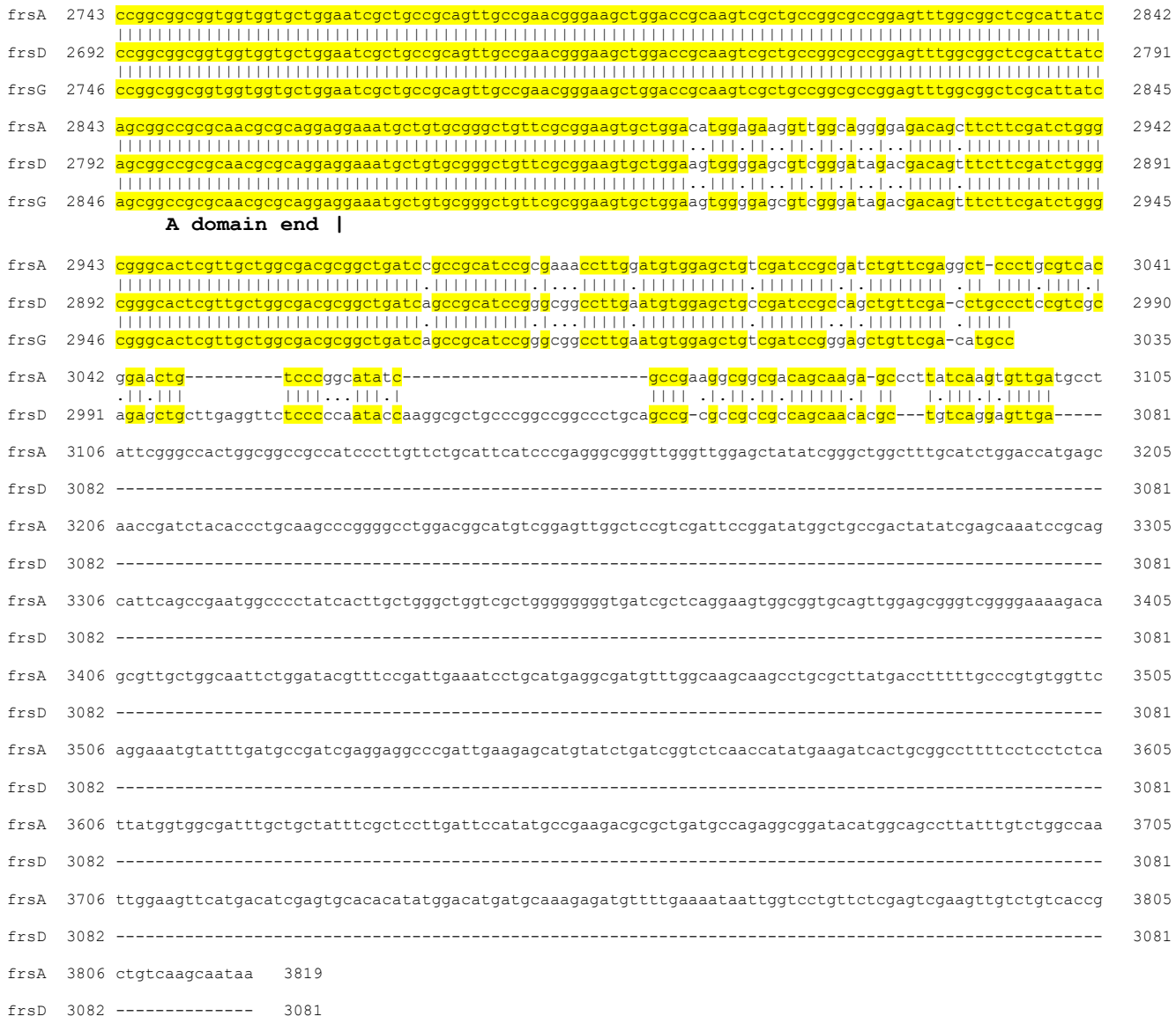

Supplementary Figure 5: Emboss Needle Alignment of *frsA* and *frsD* and the A domain encoding sequence of *frsG* (bp 1270-3035) in *C. vaccinii.* Identical base pairs are highlighted in yellow.

Supplementary Figure 6: Emboss Needle Alignment of FrsA and FrsD in *C. vaccinii*. Identical amino acids are highlighted in yellow.

Establishment of Knock-out System in *C. vaccinii* and Creation of Mutant Strains

Construction of the *frsA* and *vioA* knock-out vectors

At first, a classical multiple cloning procedure (sequential cloning) was used to generate the *C. vaccinii* MWU205 Δ*frsA* mutant. Later, a more elaborate method, based on Gibson assembly (one step cloning) was employed to delete *vioA* (Supplementary Fig. 7). For both approaches, the upstream (up) and downstream (dn) DNA sequences of the respective genes (ca. 1.1 kb for *frsA* and ca. 0.4 kb for *vioA*) were amplified by Q5 PCR with suitable primers (Supplementary Table 1). In addition the 1.8 kb FRT cassette (Gem^R Gfp^+) (FRT) from pPS858[3] was amplified by Q5 PCR. All PCR reactions were prepared in a 25 µL scale as described above with either 2–22 ng *C. vaccinii* MWU205 gDNA (*frsA* and *vioA* up- and downstream) or 0.5–4.5 ng pPS858 (FRT) as template. The fragments for sequential cloning were then cloned into pUC19[4] in a directional manner in the following order: FRT > *frsA*-up > *frsA*-dn. For this, standard restriction/ligation based cloning techniques were used. The insert of the resulting plasmid pUC19::Δ*frsA*, consisting of all three fragments, was then subcloned into pEX18Tc by using the flanking restriction sites for *Sac*I and *Sph*I. This yielded the final knock-out vector pEX18TC::Δ*frsA*. In contrast, the one step cloning approach followed the protocol of Gibson et al.[5] For this, a reaction mixture (20 µL scale) containing 4.5 nM of the PCR amplified inserts (FRT, *vioA*-up, *vioA*-dn), 1.375 nM *Bam*HI linearized pEX18Tc, 0.0054 U/µL T5 exonuclease (NEB), 0.034 U/µL Phusion polymerase (NEB), 5.4 U/µL *Taq* DNA ligase (NEB) and 1x ISO buffer (10 mM $MgCl_2$, 200 µM deoxynucleotide triphosphates, 10 mM DTT, 5% (w/v) PEG-8000, 1 mM NAD, 100 mM Tris-HCl pH 7.5) was set up. This mixture was then incubated at 50 °C for 1 h. 5 µL of this reaction mixture were then transformed into chemically competent *E. coli* NEB Turbo cells (NEB). Positive clones were initially identified by colony PCR. For this, screening reactions were performed in a 25 µL scale with 1x GoTaq reaction buffer with 1.5 mM $MgCl_2$, 4% DMSO, 200 µM dNTP, 100 nM of forward and reverse primer, DNA template (bacterial suspension in water) and GoTaq G2 DNA polymerase (0.025 U/µL, Promega). Plasmids from positive clones were then verified by restriction digest analysis as well as terminal-end Sanger sequencing. This yielded the final knock-out vector pEX18Tc::Δ*vioA*.

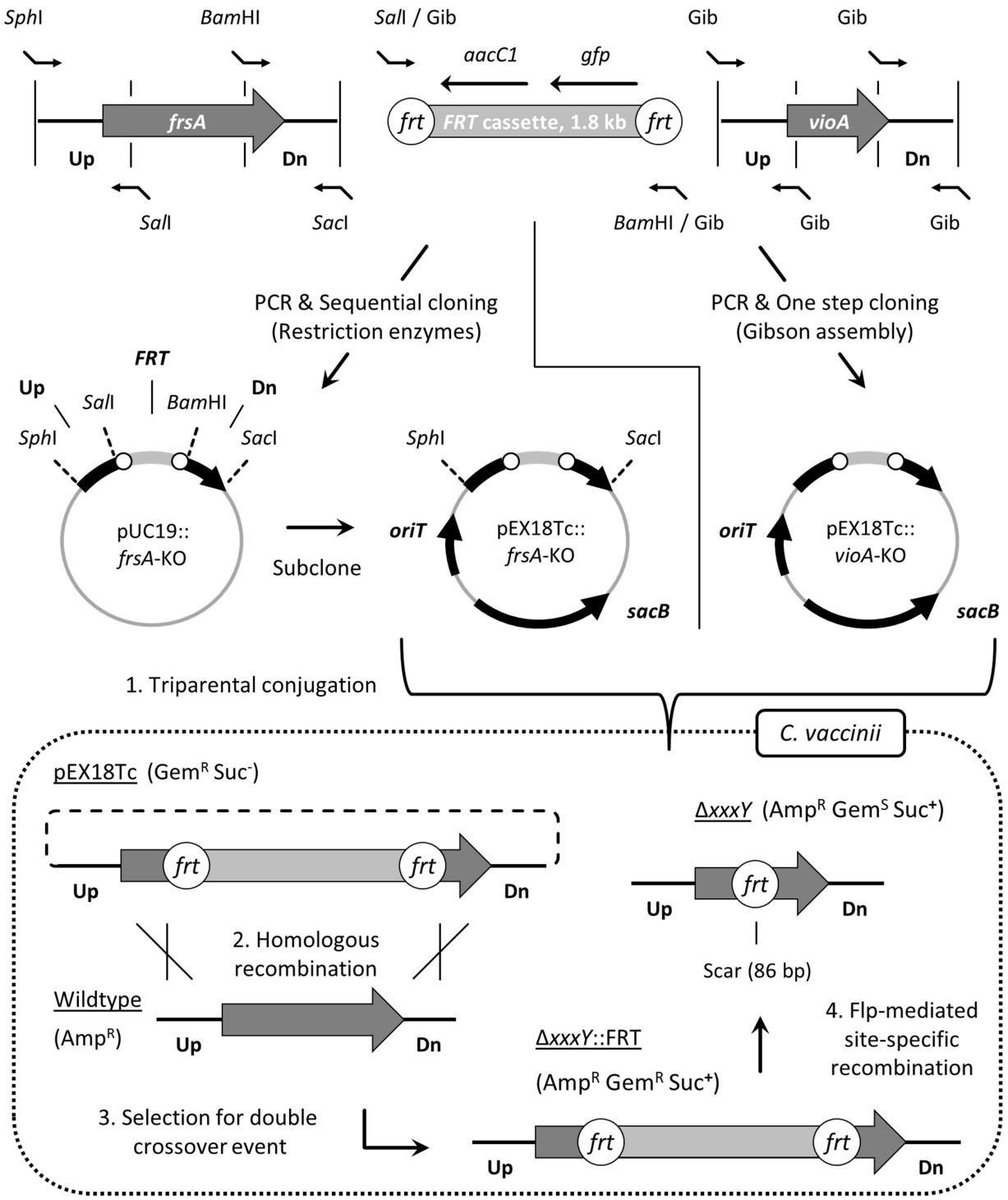

Supplementary Figure 7: Schematic representation of the deletion strategy used for *frsA* and *vioA*. This involves the construction of the knock-out vectors pEX18Tc::*frsA*-KO (sequential cloning) and pEX18Tc::*vioA*-KO (Gibson assembly) (upper half) and their use for generation of the *C. vaccinii* Δ*frsA* and Δ*vioA* deletion mutants (lower half). This involves 1. Transfer of the knock-out vectors by triparental conjugation, 2. Exchange of the targeted gene with the *FRT* cassette (*aacC1* and *gfp* flanked by two *frt* sites) by homologous recombination, 3. Selection for an exchange by double homologous recombination as well as loss of the knock-out vector and 4. Removal of the *FRT* cassette by Flp-mediated site-specific recombination between the two *frt* sites. Restriction enzyme cutting sites used for cloning as well as overhangs necessary for Gibson assembly (Gib) are indicated. For further details see respective sections in manuscript and Materials and Methods. (Δ*xxxY*::FRT = deleted gene with integrated FRT cassette; Δ*xxxY* = deleted gene with scar; Amp^R = Ampicillin resistant; Gem^R / Gem^S = Gentamicin resistant / sensitive; Suc^+ / Suc^- = Sucrose unsusceptible / susceptible).

Preparation of knockout mutants

Transfer of pEX18Tc::Δ*frsA* or pEX18Tc::Δ*vioA* into *C. vaccinii* MWU205 occurred by triparental conjugation employing *E. coli* NEBTurbo harboring one of the knockout vectors and the conjugational helper strain *E. coli* ET12567 pUB307. All three strains were grown in 15 mL LB at 30 °C, 220 rpm to an OD600 of 0.4 - 0.6. Cells were then washed two times with 10 mL LB to remove any antibiotics and were finally resuspended in an appropriate amount of LB. The resulting suspensions were then mixed in a 3:1 ratio of donor strains and acceptor strain (600 µL *E. coli* NEBTurbo with pEX18Tc::Δ*frsA* or pEX18Tc::Δ*vioA*, 600 µL *E. coli* ET12567 pUB307, 200 µL *C. vaccinii* MWU205), centrifuged (2 min, 9,000 rpm, RT) and the pellet resuspended in a small part of the supernatant (ca. 100 µL). This mixture was applied to a LB agar plate without antibiotics in the form of a 'puddle'. After drying, the plate was incubated for 24 h at 30 °C. On the next day, the resulting cell layer was scraped off and resuspended in 1 mL LB without NaCl (NS-LB). The suspension was then plated on NS-LB agar containing Amp200, Gem30 and 15% sucrose (w/v) and the plates were incubated for 60–72 h at 25 °C. Resulting clones were screened for a successful double homologous recombination event by colony PCR as described above. Three positive clones were then further tested for an integration of the FRT cassette at the right genomic locus. For this, the respective regions were amplified by Q5 PCR with primers binding outside the sequences used for construction of the knockout vectors (Supplementary Table 1, Supplementary Fig. 8a). All PCR reactions were prepared in a 25 µL scale with 75 - 200 ng of *C. vaccinii* MWU205 mutant gDNA as template as described above. Resulting PCR products which showed the expected size difference (minus 1,897 bp for Δ*frsA*::FRT, plus 879 bp for Δ*vioA*::FRT) compared to the wild type (6,144 bp for *frsA*, 2,043 bp for *vioA*) (Supplementary Fig. 8b), were purified and applied to terminal-end Sanger sequencing along with the primers used for amplification. As pUB307 is a self-transferable helper plasmid, all correct clones were routinely tested for the loss of pUB307 by plating them on kanamycin and tetracycline. Only clones, who failed to grow on either antibiotic, were considered for further usage as this indicates a loss of the plasmid. Alternatively, cells were cured from pUB307 by growing them in LB supplemented with 5 % (w/v) SDS at 30 °C for 24–48 h and replating them on selective agar. To remove the FRT cassette from the genome of the *C. vaccinii* Δ*frsA*::FRT or Δ*vioA*::FRT deletion mutants, the genes *flp* and *sacB* from pFlp2[3] were introduced into the broad host vector pBMTL-2[6] as described by Wang et al.[7] The resulting vector pBMTL-2::*flp-sacB* was then transferred to the deletion mutants by electroporation following the protocol established for *Chromobacterium violaceum*.[8] After the transformation clones were grown overnight at 30 °C, which has been shown to be sufficient for FRT removal by Flp mediated site specific recombination.[3] Positive clones that lost the FRT cassette were identified by colony PCR and plated on NS-LB with Amp200 and 15% sucrose (w/v) to remove the pBMTL-2::*flp* plasmid. Loss of the plasmid was then confirmed by colony PCR as well as testing the clones for kanamycin susceptibility. To verify modification of the correct genomic locus, three clones were further investigated by Q5 PCR as described above. In this case, removal of the FRT cassette was indicated by the formation of a smaller

PCR product (loss of 1,725 bp) compared to the mutants with FRT cassette. The mutants verified in this manner were termed *C. vaccinii* MWU205 Δ*frsA* and *C. vaccinii* MWU205 Δ*vioA*, respectively. The double mutant *C. vaccinii* MWU205 Δ*frsA*/Δ*vioA* was constructed as described above by using *C. vaccinii* MWU205 Δ*frsA* as starting strain. Mutant strains were grown and extracted analogous to the wild type strain (see above).

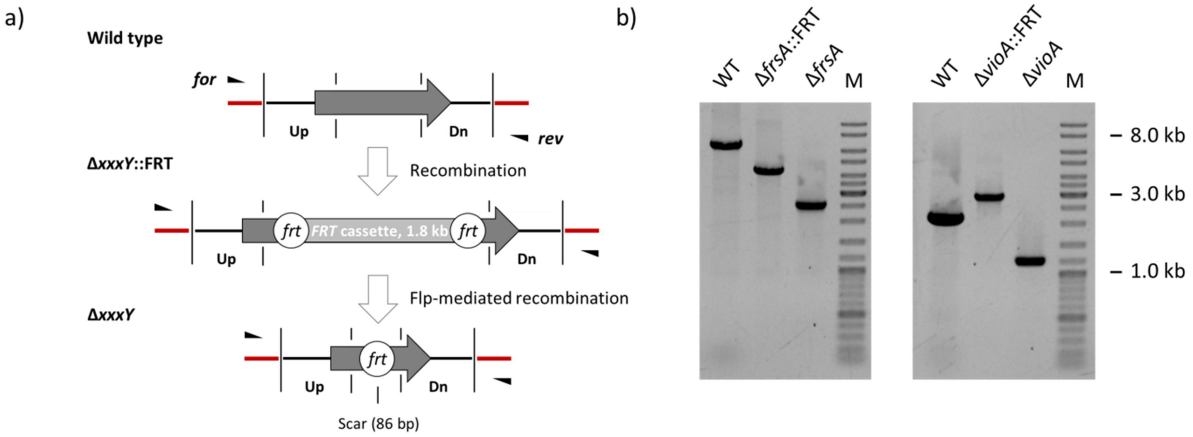

Supplementary Figure 8: Verification of *C. vaccinii* deletion mutants. a) PCR-based genotype verification applied during the construction of markerless *C. vaccinii* deletion mutants. All primers used for amplification (for/rev) bind to the regions outside the sequences used for knock-out vector construction (Up/Dn), which are shown here in red. This ensures a modification at the right locus. b) Q5-PCR of the *C. vaccinii* wild type as well as the different deletion mutants (Δ*frsA*::FRT, Δ*frsA*, Δ*vioA*::FRT, Δ*vioA*) with the respective verification primers (PCR-frsA_for/rev or PCR-vioA_for/rev). PCRs performed with the same primer pairs for the *C. vaccinii* Δ*frsA*/Δ*vioA* double mutant yielded identical results as for the single knock-out mutants. (ΔxxxY::FRT = deleted gene with integrated FRT cassette; ΔxxxY = deleted gene with scar). These experiments were independently repeated at least three times with similar results.

Structure elucidation of FR-Core (2)

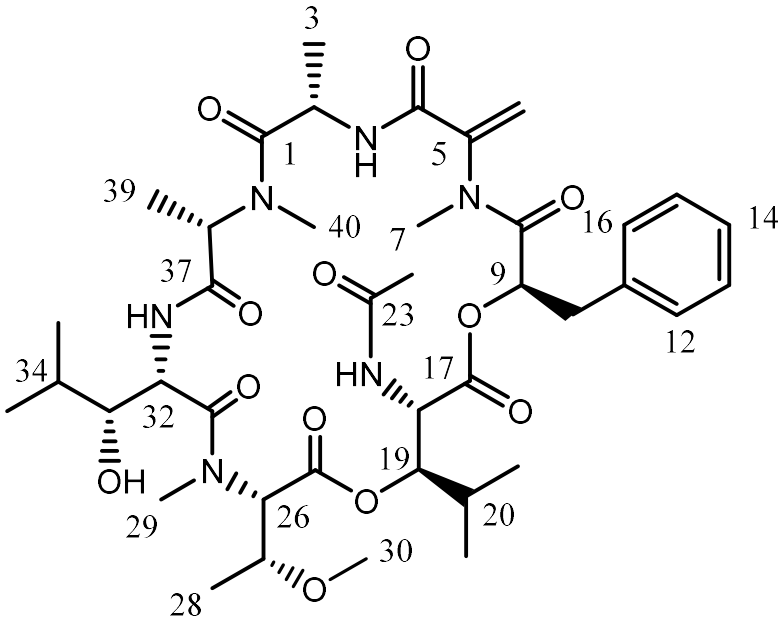

Supplementary Figure 9: Chemical structure of FR-Core (**2**). Carbon atoms are numbered.

Supplementary Table 4: ^{1}H and ^{13}C NMR spectroscopic data of **2** (see Supplementary Figure 9) in acetonitrile-d_3 (^{1}H: 600 MHz; ^{13}C: 150 MHz).

Residue[a]	No C/H	δ_C, mult	δ_H (*J* [Hz])
Ala	1	172.5, C	–
	2	44.3, CH	5.11 (dq, 9.1, 6.7)
	2-NH	–	7.12 (d, 9.1)
	3	16.7, CH_3	1.19 (d, 6.7)
N-Me-Dha	4	162.2, C	–
	5	142.1, C	–
	6a	122.8, CH_2	a 5.62 (br s)
	6b	–	b 3.60 (br s)
	7	36.6, CH_3	2.89 (s)
Pla	8	168.5, C	–
	9	71.6, CH	5.56 (dd, 4.3, 10.5)
	10a	38.5, CH_2	a 3.15 (dd, 4.3, 12.5)
	10b	–	b 3.10 (dd, 10.5, 12.5)
	11	136.3, C	–
	12/16	130.5, CH	7.24[b]
	13/15	128.9, CH	7.29[b]
	14	127.5, CH	7.27[b]
N-Ac-*β*-OH-Leu	17	169.7, C	–
	18	53.1, CH	4.91 (dd, 2.2, 9.6)
	18-NH	–	6.88, (d, 9,6)
	19	78.3, CH	5.41 (br d, 10.0)
	20	30.4, CH	1.79 (m)
	21	18.6, CH_3	0.83 (d, 6.8)
	22	18.1, CH_3	0.87 (d, 6.8)
	23	170.5, C	–

	24	22.4, CH_3	2.02 (s)
N,O-Me_2-Thr	25	168.1, C	–
	26	67.9, CH	3.55 (d, 9.8)
	27	74.1, CH	3.95 (dq, 9.8, 5.9)
	28	17.8, CH_3	1.26 (d, 5.9)
	29	40.0, CH_3	3.23 (s)
	30	56.5, CH_3	3.27 (s)
β-OH-Leu	31	170.5, C	–
	32	50.3, CH	4.95 (dd, 6.9, 10.4)
	32-NH		6.94, (d, 10.4)
	33	77.1, CH	3.42 (br t, 5.8)
	34	28.8, CH	1.93 (m)
	35	20.3, CH_3	1.02 (d, 6.7)
	36	15.6, CH_3	0.93 (d, 6.7)
N-Me-Ala	37	169.6, C	–
	38	61.4, CH	3.61 (q, 6.7)
	39	12.3, CH_3	1.38 (d, 6.7)
	40	38.0, CH_3	3.17 (s)

[a] Residues: Ala = alanine, *N*-Me-Dha = *N*-methyldehydroalanine, Pla = 3-phenyllactic acid, *N*-Ac-*β*-OH-Leu= *N*-acetyl-3-hydroxyleucine, *N*,*O*-Me_2-Thr = *N*,*O*-dimethylthreonine, *β*-OH-Leu = 3-hydroxyleucine, *N*-Me-Ala = *N*-methylalanine,. [b] overlapping resonances.

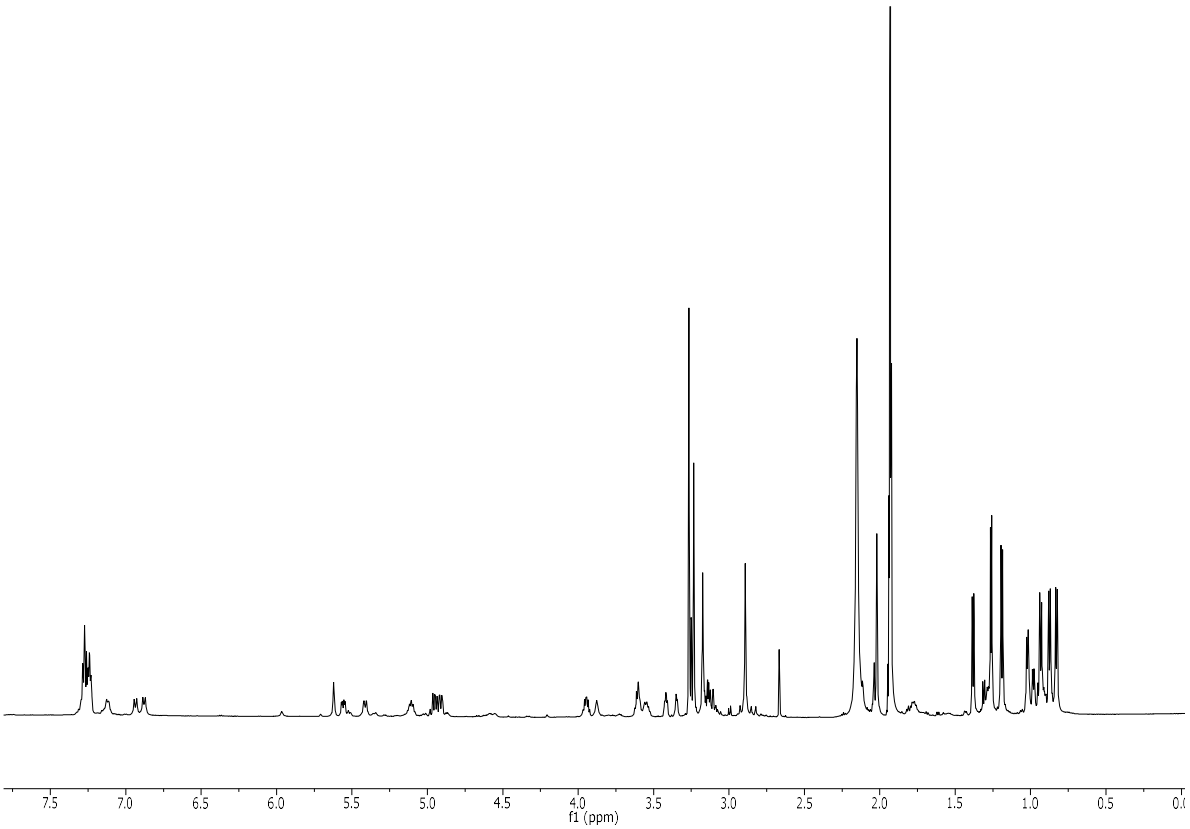

Supplementary Figure 10: ^{1}H NMR spectrum of compound **2** in acetonitrile-d_3 (600 MHz).

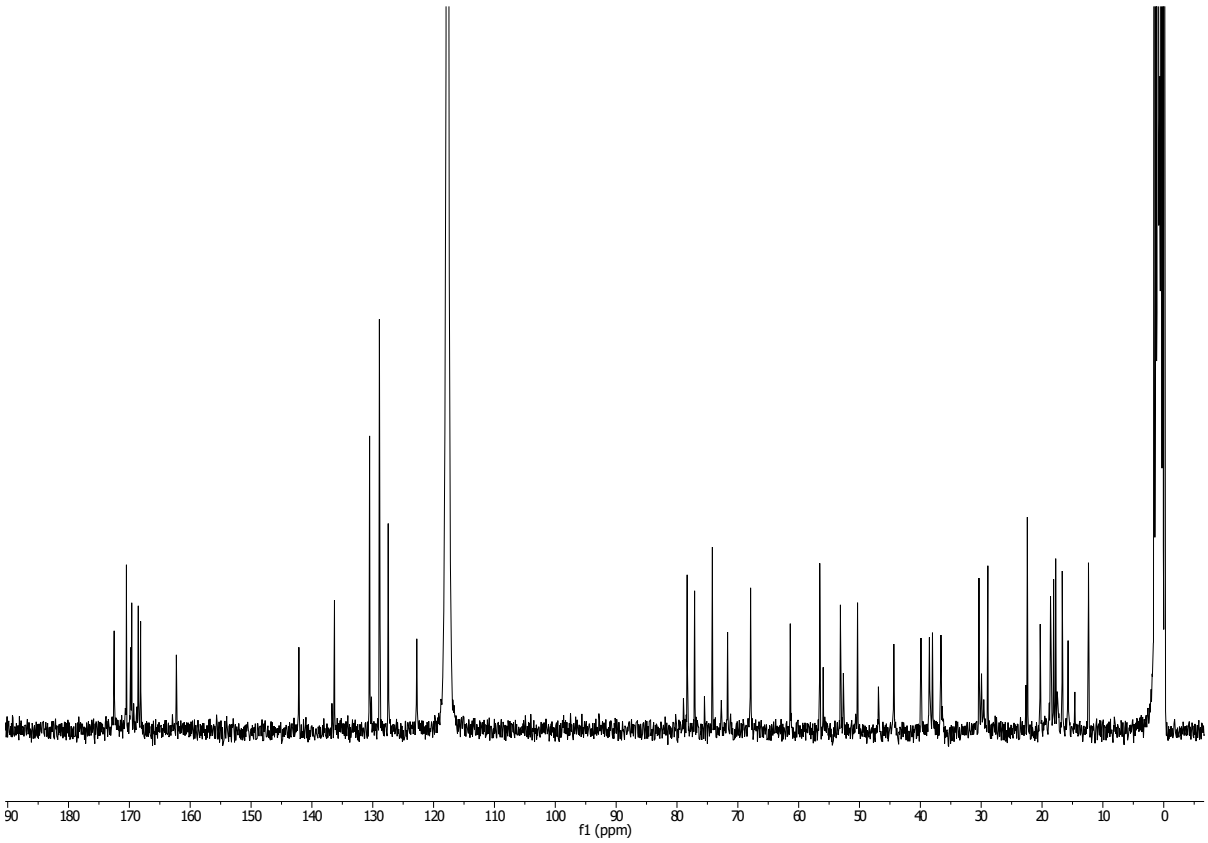

Supplementary Figure 11: ^{13}C NMR spectrum of compound **2** in acetonitrile-d_3 (150 MHz).

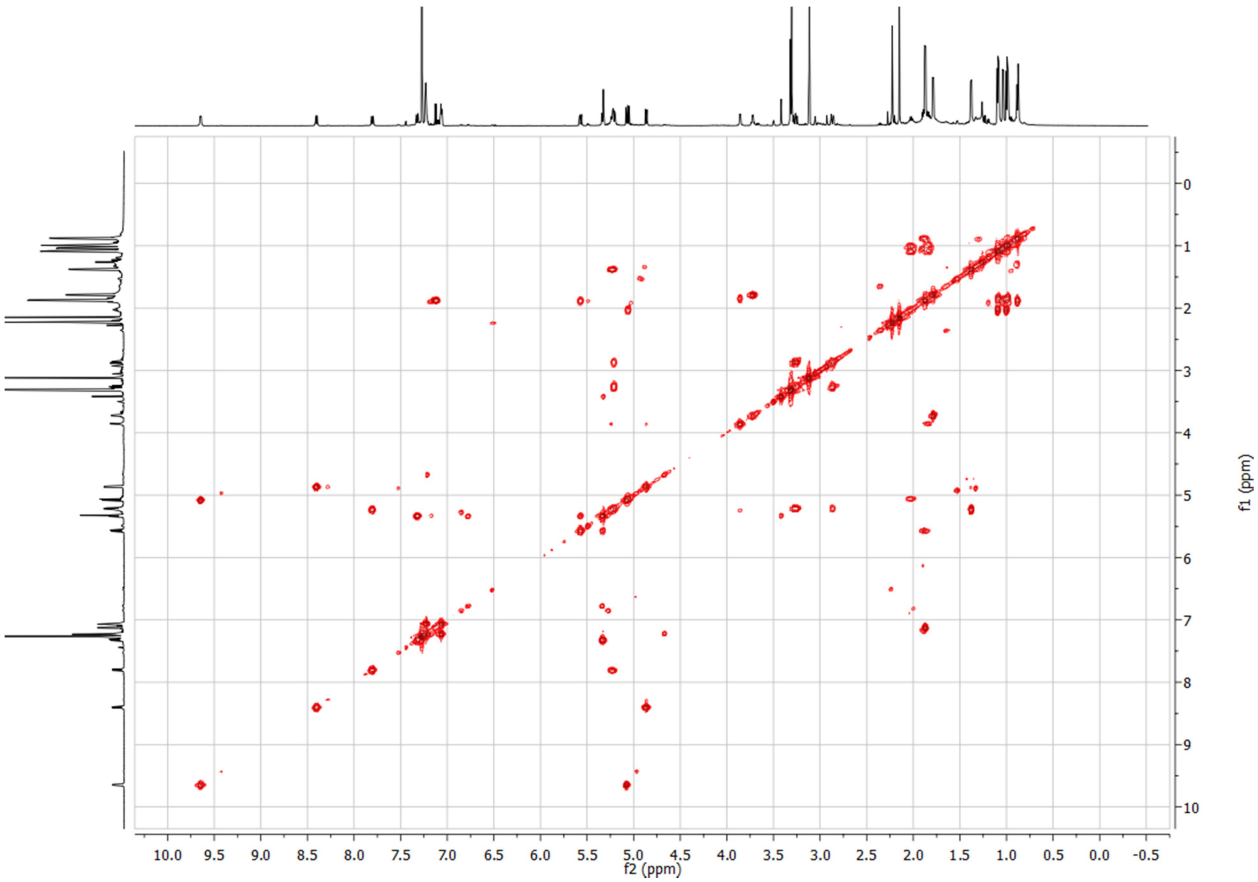

Supplementary Figure 12: ^{1}H-^{1}H COSY NMR spectrum of compound **2** in acetonitrile-d_3 (600 MHz).

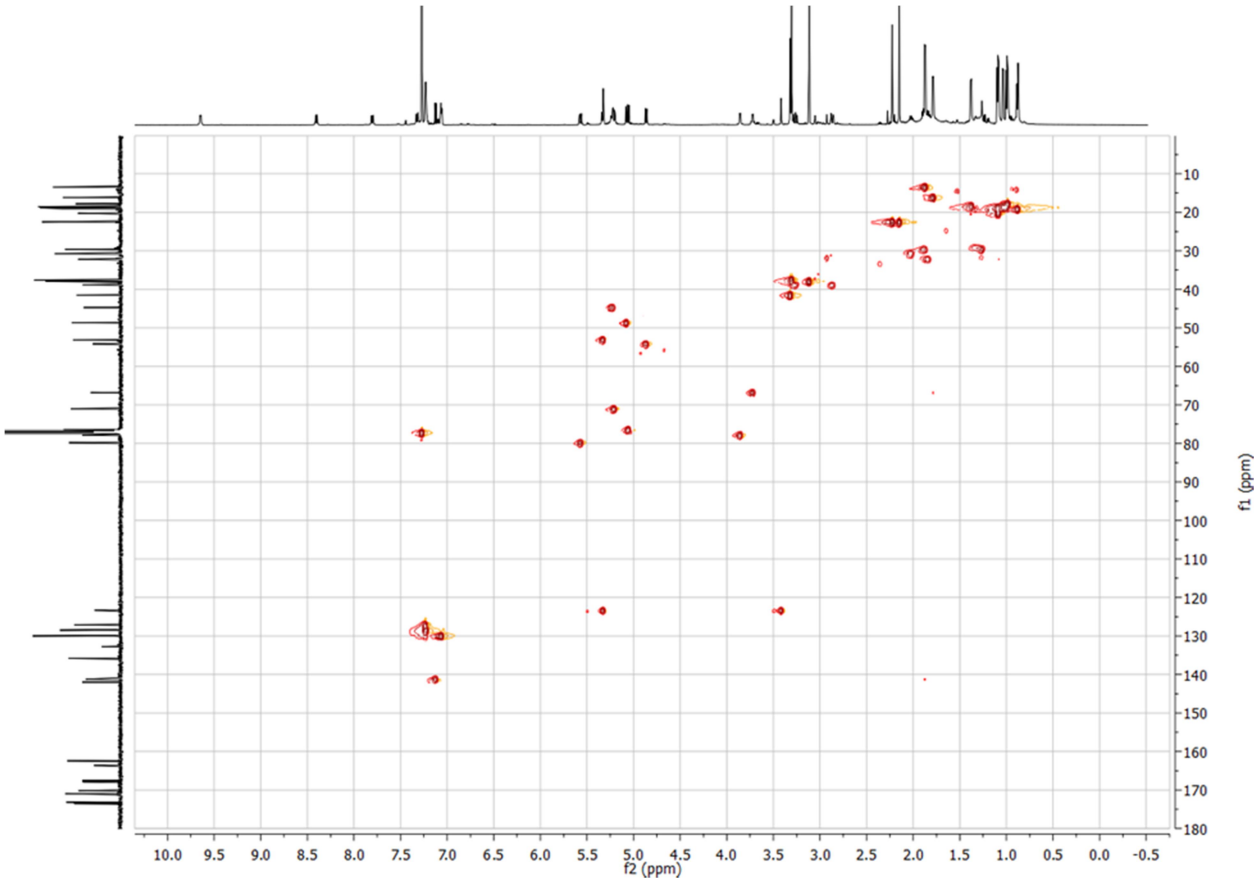

Supplementary Figure 13: ^{1}H-^{13}C HSQC NMR spectrum of compound **2** in acetonitrile-d_3 (600 MHz).

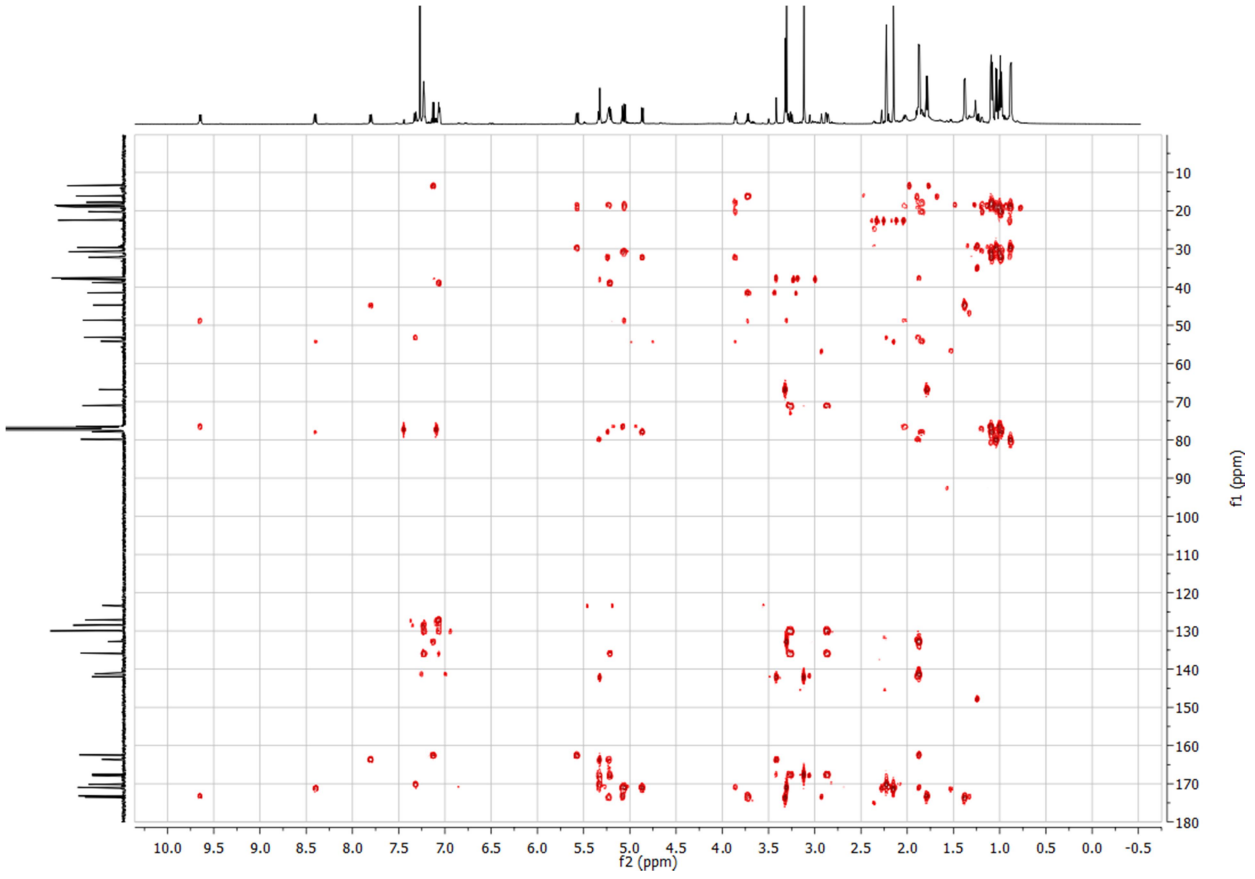

Supplementary Figure 14: ^{1}H-^{13}C HMBC NMR spectrum of compound **2** in acetonitrile-d_3 (600 MHz).

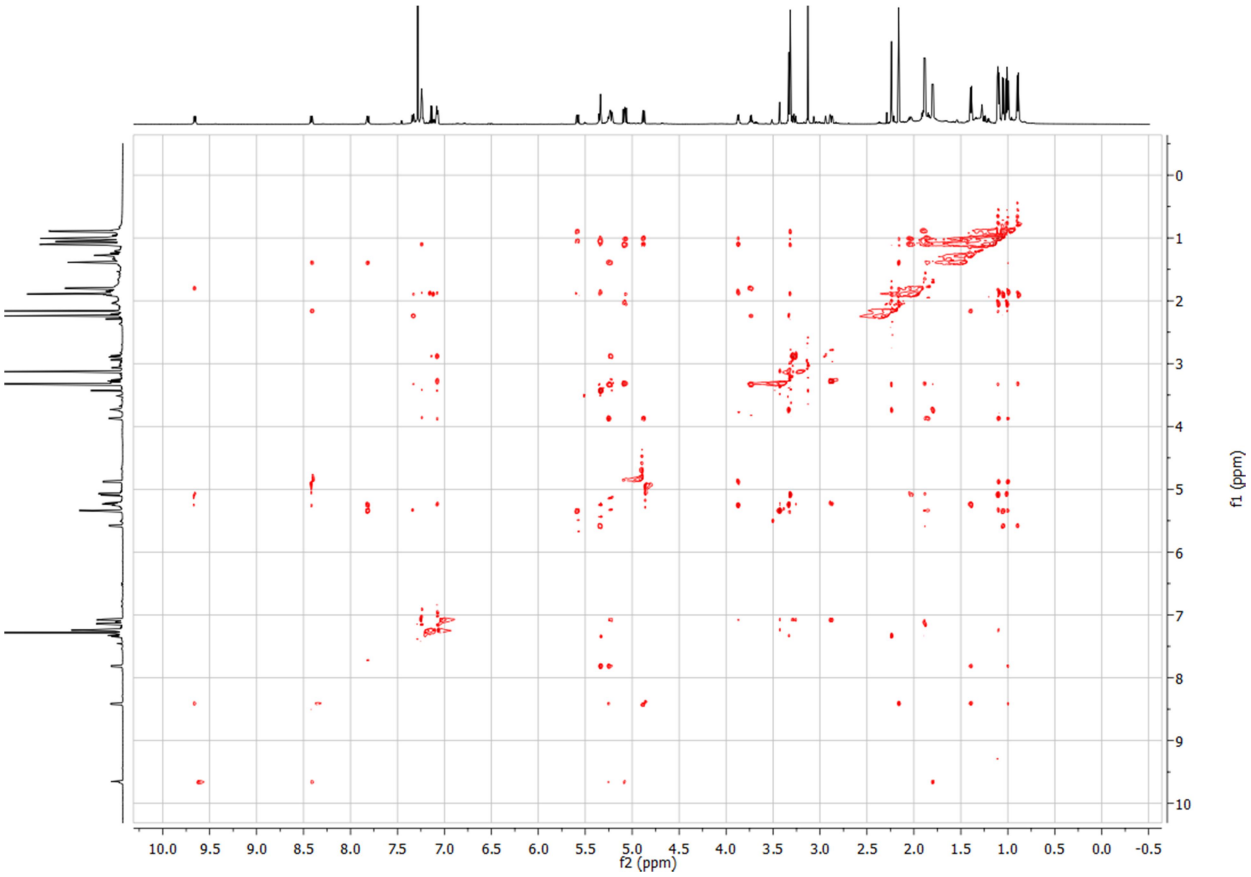

Supplementary Figure 15: ^{1}H-^{1}H ROESY NMR spectrum of compound **2** in acetonitrile-d_3 (600 MHz)

In vitro Characterization of NRPS Domains and FrsH

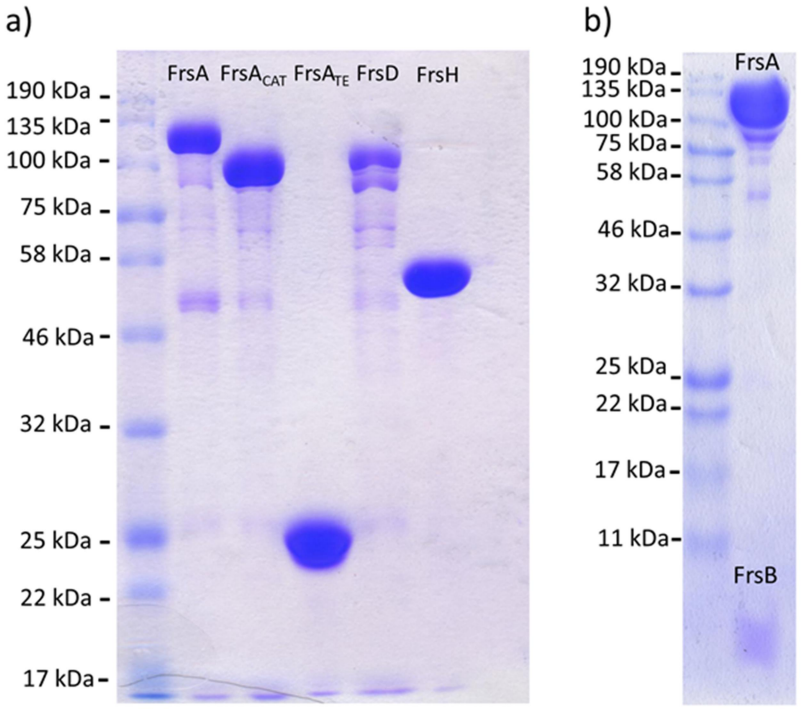

Supplementary Figure 16: a) SDS-PAGE gel of FrsA, FrsD and FrsH constructs. FrsA and FrsD were always coexpressed with the MbtH-like protein FrsB (not visible on the a) gel), which was crucial for solubility and activity of the NRPS proteins. These experiments were independently repeated at least three times with similar results. **b) SDS-PAGE gel of coexpressed FrsA and FrsB.** The FrsB, expressed without His_6-tag, coelutes in approximately 1:1 molar ratio with FrsA and is visible in SDS buffer systems for small proteins, Size FrsB: 8.12 kDa. These experiments were independently repeated at least three times with similar results.

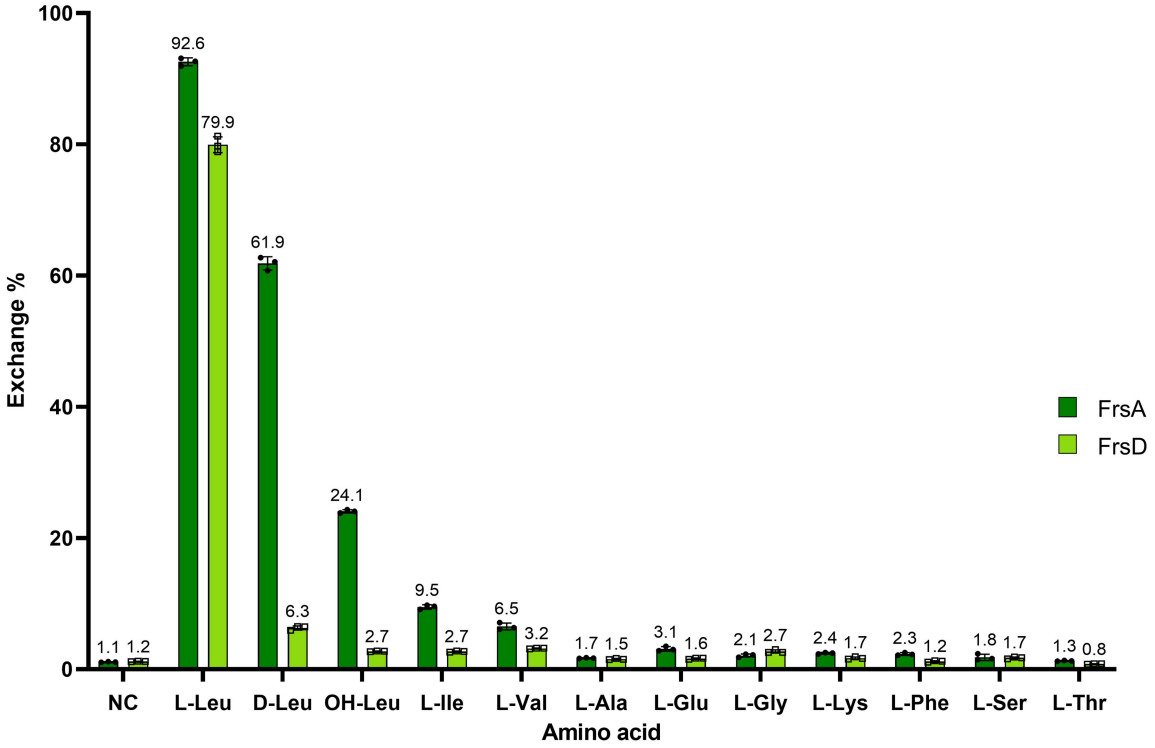

Supplementary Figure 17: $^{18}O_4$-ATP exchange adenylation assay results for FrsA and FrsD, both coexpressed with FrsB. Data are presented as mean values ± SD. All experiments were performed in triplicate.

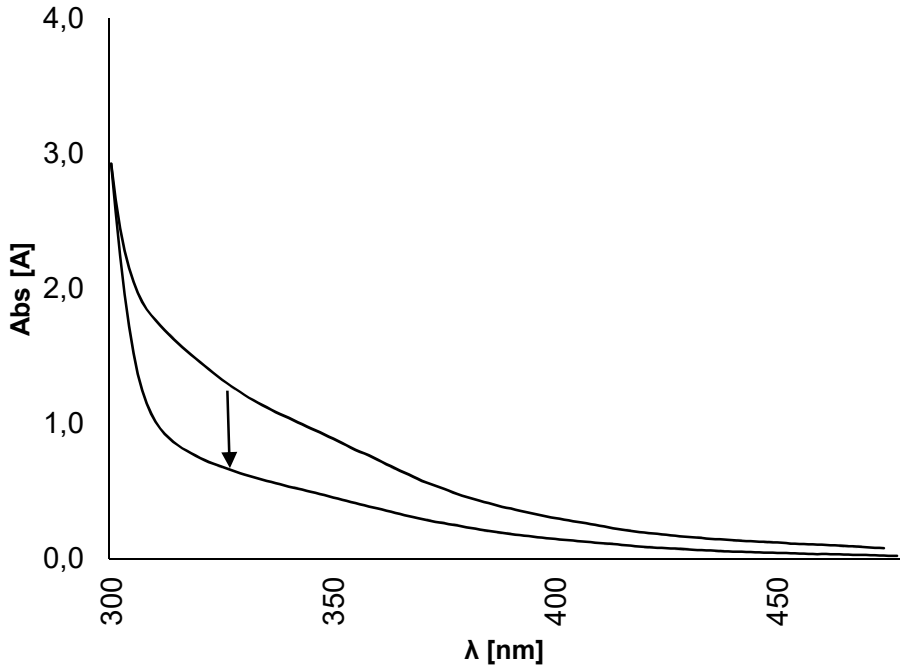

Supplementary Figure 18: Absorption spectra of FrsH. The iron cluster is visible as a broad feature between 300 – 400 nm in the ferrous state. Reduction to the ferric state diminishes the feature.

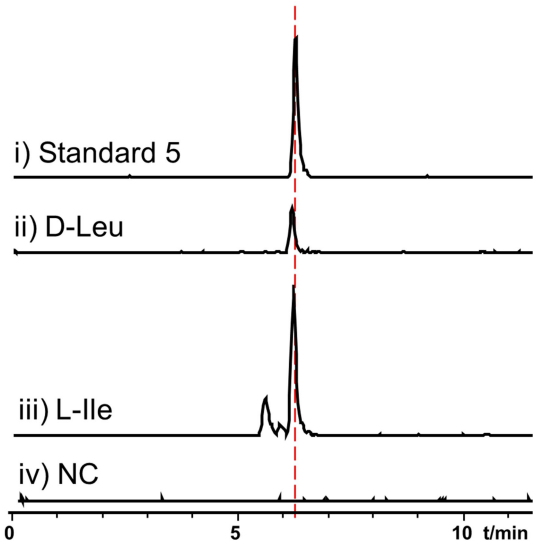

Supplementary Figure 19: EIC (*m/z* = 202.108) showing production of **5**. i) **5**, 1 µg/mL. ii) Enzymatic assay with purified $FrsA_{CAT}$/FrsB, FrsH, incubated with D-Leu and propionyl-CoA, hydrolyzed with KOH. iii) Enzymatic assay with L-Ile v) negative control with heat inactivated proteins.

Chemical synthesis of compounds 5 and 6

General Procedures

Thin-layer chromatography was carried out on Merck (Darmstadt, Germany) aluminium sheets, silica gel 60 F254. Detection was performed with UV light at 254 nm. Preparative column chromatography was performed on Merck silica gel (0.063-0.200 mm, 60 Å). Melting points were determined on a Büchi (Essen, Germany) 510 oil bath apparatus. ^{1}H NMR (500 MHz) and ^{13}C NMR (125 MHz) spectra were recorded on a Bruker Avance DRX 500. Chemical shifts δ are given in ppm referring to the signal centre using the solvent peaks for reference: DMSO-d_6 2.49/39.7 ppm. LC-MS analyses were carried out on an API2000 (Applied Biosystems, Darmstadt, Germany) mass spectrometer coupled to an Agilent (Santa Clara, CA, USA) 1100 LC system using a EC50/2 Nucleodur C18 Gravity column (Macherey-Nagel, Düren, Germany; 50 × 2.0 mm, particle size 3 µm). Purity of the compounds was determined using the diode array detector (DAD) of the LC-MS instrument between 200 and 400 nm. HRMS were recorded on a microTOF-Q (Bruker, Köln, Germany) mass spectrometer connected to a Dionex (Thermo Scientific, Braunschweig, Germany) Ultimate 3000 LC via an ESI interface using a Nucleodur C_{18} Gravity column (50 × 2.0 mm I.D., 3 µm, Macherey-Nagel, Düren, Germany).

(2*S*,3*R*)-3-Hydroxy-4-methyl-2-propionamidopentanoic acid (5).

A stirred solution of propanoic acid (370 mg, 5.00 mmol) and *N*-methylmorpholine (506 mg, 5.00 mmol) in THF (8.6 mL) was cooled to -10 °C. Isobutyl chloroformate (683 mg, 5.00 mmol) was added and the reaction was allowed to stir for 0.5 h. The temperature was adjusted to 0 °C, followed by treatment with (2*S*,3*R*)-2-amino-3-hydroxy-4-methylpentanoic acid (1.10 g, 7.50 mmol) in 1 M NaOH (5.2 mL). Since excess of base was avoided, racemization was prevented After stirring the reaction for further 24 h at room temperature, the mixture was diluted with H_2O (16 mL) and washed with ethyl acetate (2 × 16 mL). The combined ethyl acetate layer was extracted with sat. aq. $NaHCO_3$ solution (3 × 16 mL). All aqueous layers were combined, adjusted to pH ~2 by adding 1 M HCl and extracted with ethyl acetate (3 × 32 mL). This combined organic layer was dried over Na_2SO_4, filtered and evaporated to dryness. The crude residue was purified by column chromatography on silica gel using a gradient of petroleum ether/ethyl acetate (1:1) + 1% AcOH to 100% ethylacetate + 1% AcOH to give a white solid (762 mg, 75%); mp 104–106 °C.

^{1}H NMR (500 MHz, DMSO-d_6) δ 0.77 (d, ^{3}J = 6.7 Hz, 3H) and 0.90 (d, ^{3}J = 6.6 Hz, 3H, CH(CH_3)$_2$), 0.98 (t, ^{3}J = 7.6 Hz, 3H, CH_2CH_3), 1.50 – 1.58 (m, 1H, CH(CH$_3$)$_2$), 2.12 – 2.20 (m, 2H, CH_2), 3.50 (dd, ^{3}J = 8.7 Hz, ^{3}J = 2.8 Hz, 1H, CH-OH), 4.40 (dd, ^{3}J = 9.1 Hz, ^{3}J = 2.8 Hz, 1H, CH-NH), 7.53 (d, ^{3}J = 9.1 Hz, 1H, NH). Two proton signals (CO_2H, OH) do not appear. ^{13}C NMR (125 MHz, DMSO-d_6) δ 10.08 (CH_2CH_3), 19.12, 19.21 (CH(CH_3)$_2$), 28.48 (*C*H(CH$_3$)$_2$), 30.92 (*C*H$_2$*C*H$_3$), 54.54 (CHNH), 76.18 (CHOH), 173.09, 173.30 (CO_2H, CONH). LC-MS (ESI) (90% H_2O to 100% MeOH in 10 min, then 100% MeOH for 10 min, DAD 196–400 nm), *m/z* = 204.0 ([M+H]$^+$).

(2*S*,3*R*)-*S*-2-Acetamidoethyl 3-hydroxy-4-methyl-2-propionamidopentanethioate (6).

(2*S*,3*R*)-3-Hydroxy-4-methyl-2-propionamidopentanoic acid (**5**, 610 mg, 3.00 mmol) was dissolved in anhydrous acetonitrile (120 mL) under nitrogen atmosphere. A solution of DCC (650 mg, 3.15 mmol) and HOBt × H_2O (482 mg, 3.15 mmol) in acetonitrile (120 mL) was slowly added, followed by *N*-acetylcysteamine (375 mg, 3.15 mmol). The reaction mixture was stirred at room temperature for 24 h. Subsequently, the urea was filtered off and the filtrate was evaporated to dryness. The crude residue was purified by preparative column chromatography using ethyl acetate/MeOH (9:1) as eluent to obtain clear oil (82 mg, 9%).

^{1}H NMR (500 MHz, DMSO-d_6) δ 0.74 (d, ^3J = 6.7 Hz, 3H) and 0.90 (d, ^3J = 6.6 Hz, 3H, CH(CH_3)$_2$), 1.02 (t, ^3J = 7.6 Hz, 3H, CH_2CH_3), 1.53 – 1.61 (m, 1H, CH(CH$_3$)$_2$), 1.78 (s, 3H, $COCH_3$), 2.26 (q, ^3J = 7.6 Hz, 2H, CH_2CH$_3$), 2.79 – 2.89 (m, 2H, CH_2S), 3.08 – 3.19 (m, 2H, NHCH_2), 3.59 (ddd, ^3J = 9.1 Hz, ^3J = 6.9 Hz, ^3J = 2.4 Hz, 1H, CHOH), 4.54 (dd, ^3J = 8.9 Hz, ^3J = 2.4 Hz, 1H, CHNH), 5.01 (d, ^3J = 6.9 Hz, 1H, OH), 7.98 (t, ^3J = 5.7 Hz, 1H, NHCH$_2$), 8.08 (d, ^3J = 8.9 Hz, 1H, CHNH). ^{13}C NMR (125 MHz, DMSO-d_6) δ 9.90 (CH_2CH_3), 18.83, 19.17 (CH(CH_3)$_2$), 22.66 (CH_3CO), 27.99 (SCH_2), 28.39 (CH(CH$_3$)$_2$), 30.99 (CH_2CH$_3$), 38.24 ($NHCH_2$), 61.53 (CHNH), 76.00 (CHOH), 169.44 (H_3CCONH), 174.03 (CH_2CONH), 201.86 (COS). LC-MS (ESI) (90% H_2O to 100% MeOH in 10 min, then 100% MeOH for 10 min, DAD 220–400 nm), *m/z* = 305.0 ([M+H]$^+$). HRMS, calcd. for $C_{13}H_{24}N_2O_4S$: [M+H]$^+$ *m/z* 305.1530; found: 305.1544.

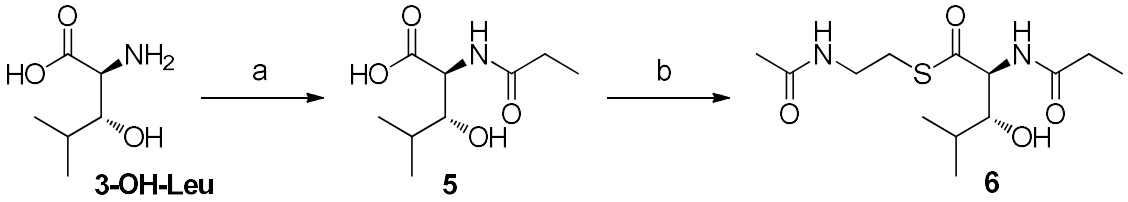

3-OH-Leu **5** **6**

Supplementary Figure 20: Synthesis of the *N*-Pp-Hle SNAC thioester **6**. Reagents and conditions: (a) propanoic acid, $ClCO_2i$-Bu, NMM, THF, 1M NaOH, -10 °C (0.5 h) to rt (24 h); (b) N-acetylcysteamine, DCC, HOBt × H_2O, MeCN, rt, 24 h, N_2.

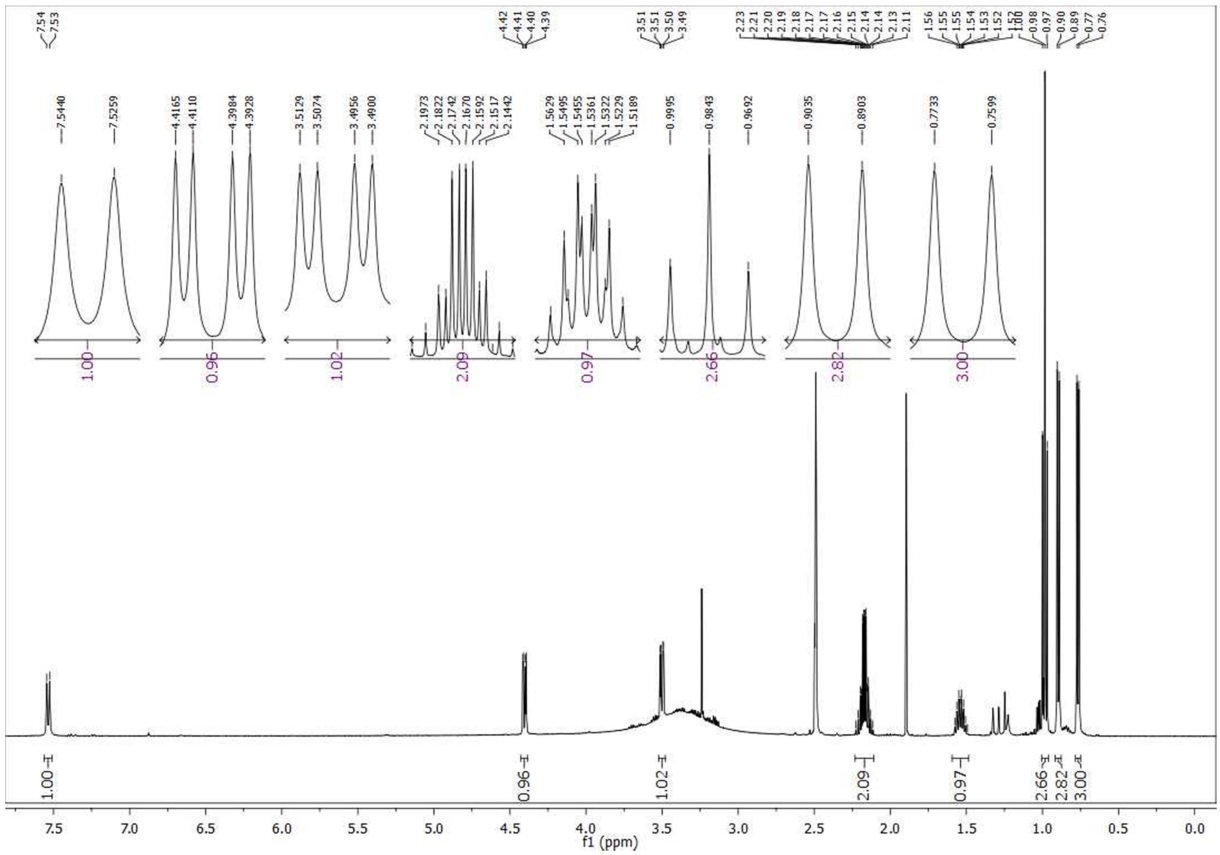

Supplementary Figure 21: ^{1}H NMR spectrum of compound **5** in DMSO-d_6 (500 MHz).

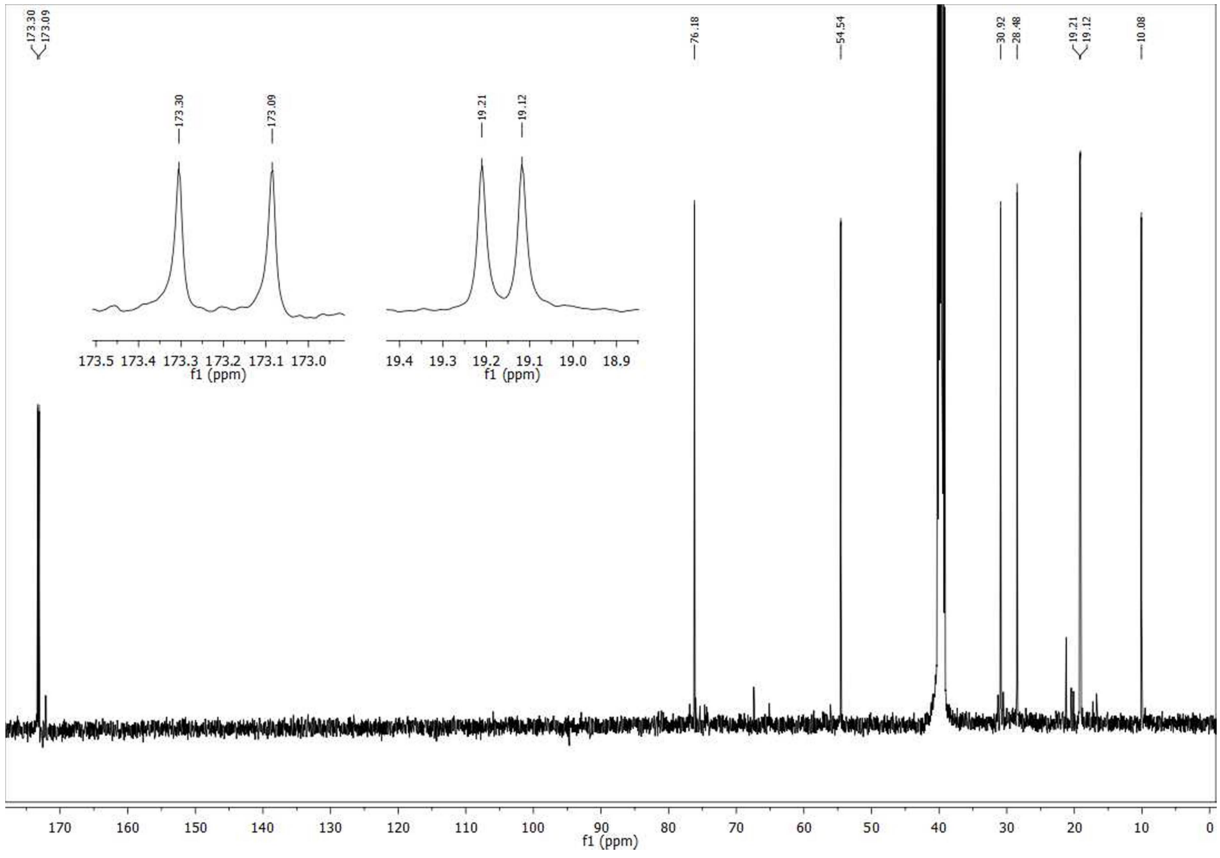

Supplementary Figure 22: ^{13}C NMR spectrum of compound **5** in DMSO-d_6 (125 MHz).

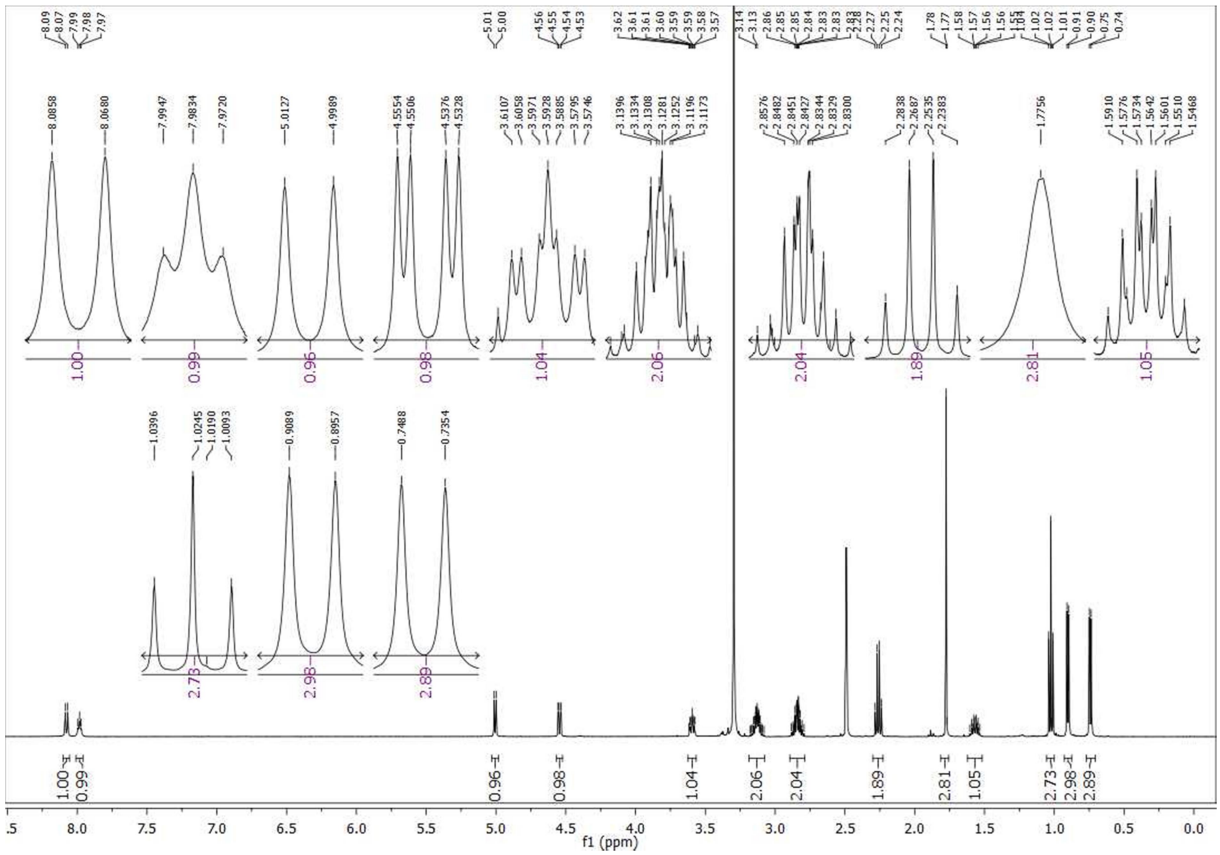

Supplementary Figure 23: ^{1}H NMR spectrum of compound **6** in DMSO-d_6 (500 MHz).

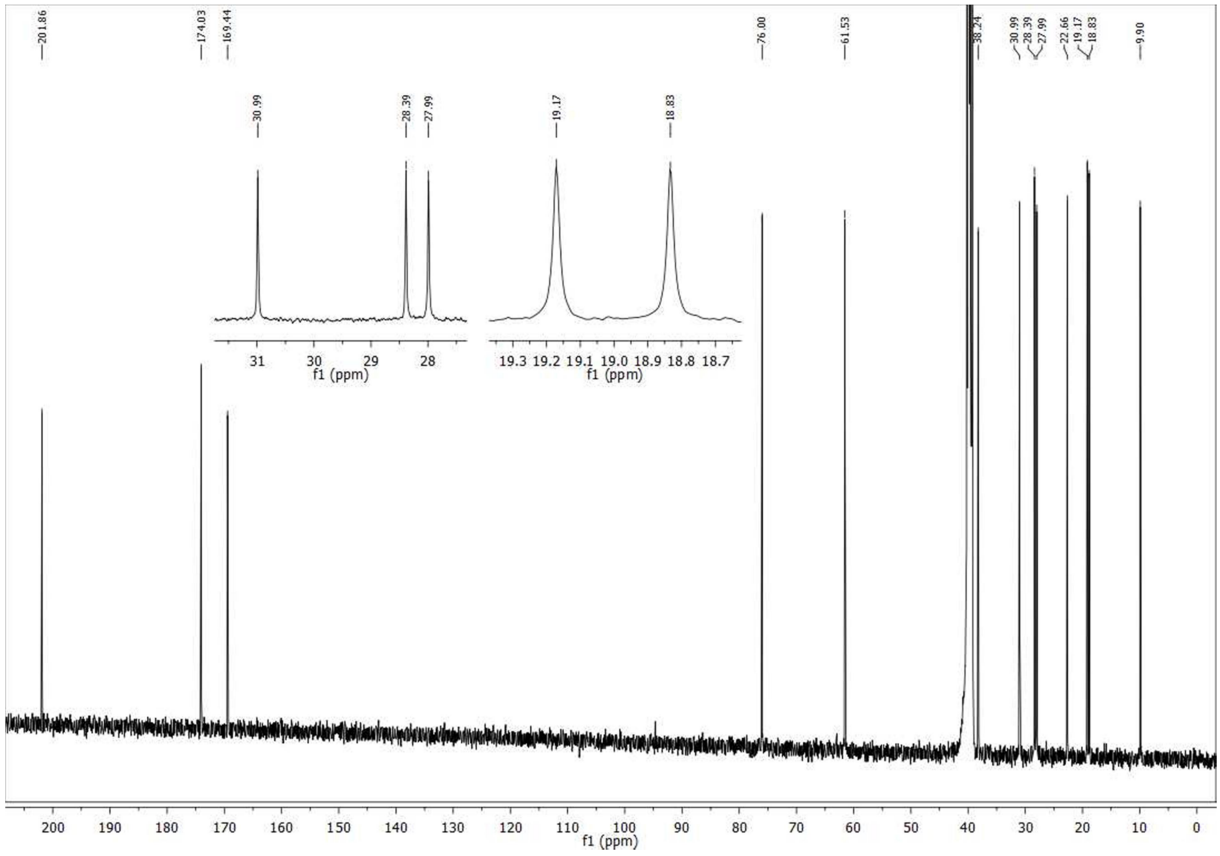

Supplementary Figure 24: ^{13}C NMR spectrum of compound **6** in DMSO-d_6 (125 MHz).

Structure Elucidation of FR-5 (7)

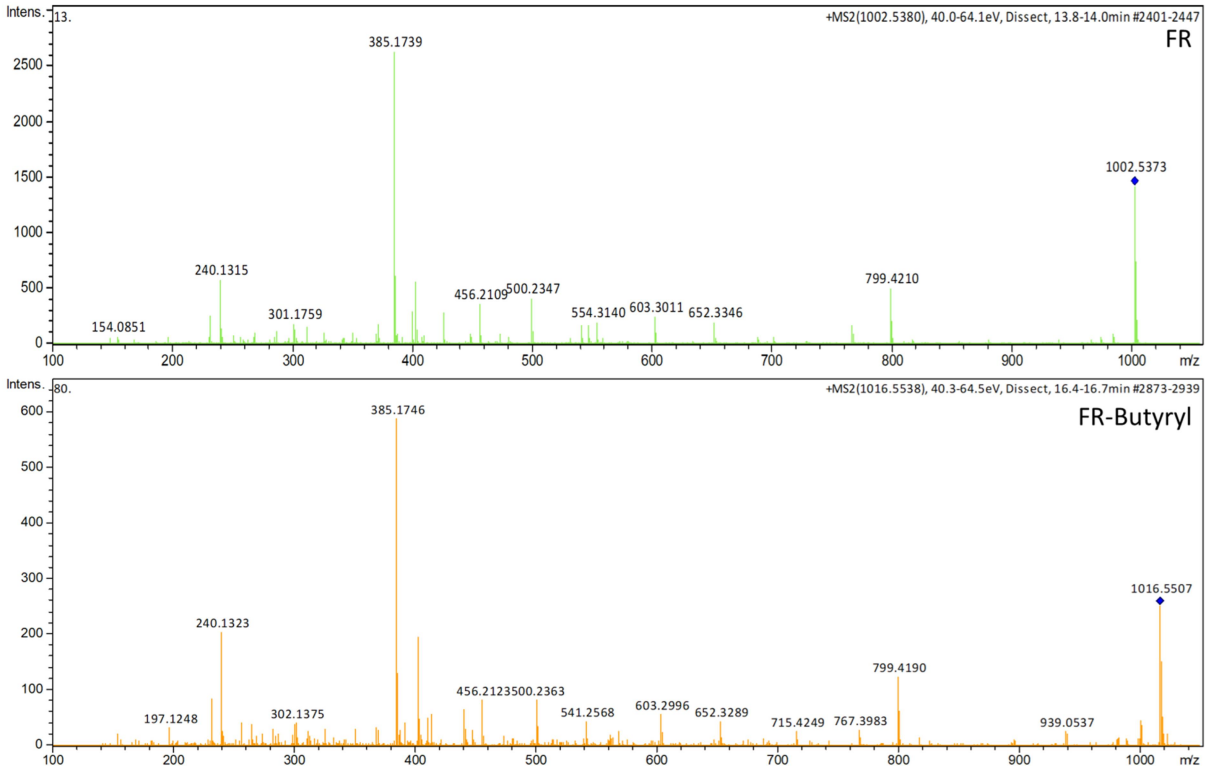

Supplementary Figure 25: MS/MS spectra of 1 (*m/z:* 1002.54) and 7 (*m/z*: 1016.55). From *m/z:* 799.42 (loss of side chain, and loss of H_2O, see Ref. 9), the compounds have the same fragmentation pattern, indicating, that the methylation of FR (M+14 Da) is in the side chain and stems most likely from the incorporation of a butyryl group from the precursor butyryl-CoA instead of the propionyl residue in FR.

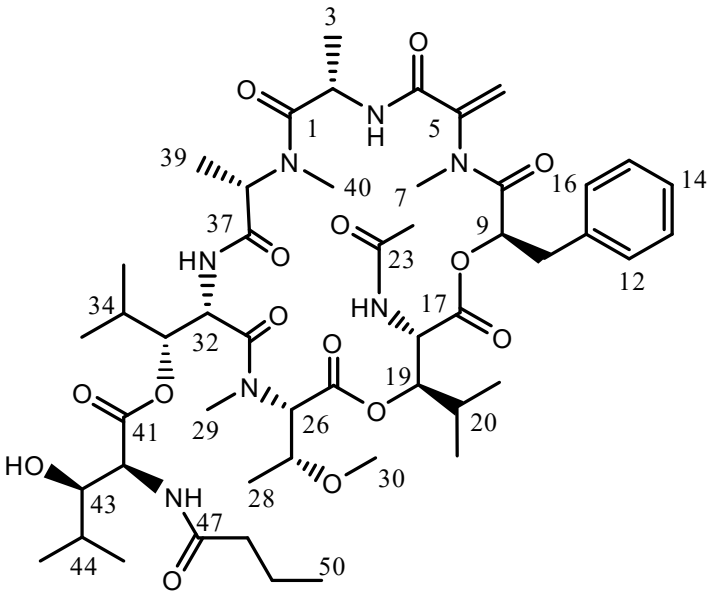

Supplementary Figure 26: **Chemical structure of FR-5** (**7**). Carbon atoms are numbered.

Supplementary Table 5: ^{1}H and ^{13}C NMR spectroscopic data of compound **7** in $CDCl_3$ (^{1}H: 300 MHz; ^{13}C: 75 MHz).

Residue[c]	No C/H[b]	δ_C[a], mult	δ_H[a] (mult, *J* in Hz)	COSY	HMBC
Ala	1	172.5, C	–		
	2	45.7, CH	4.90 (m)	3, 2-NH	1, 3, 4
	2-NH	–	8.53 (d, 9.1)	2	2, 4
	3	18.0, CH_3	1.38 (d, 6.7)	2	1, 2
N-MeDha	4	163.9, C	–		
	5	145.3, C	–		
	6	106.7, CH_2	a 5.31 (brs)	6b	5
		–	b 5.07 (brs)	6a	5
	7	36.2, CH_3	3.13 (s)		5, 8
D-Pla	8	167.7, C	–		
	9	72.6, CH	5.20 (dd, 4.2, 8.3)	10a, 10b	8, 10, 17
	10	36.6, CH_2	a 3.08 (dd, 4.2, 14.8)	9, 10b	9, 11, 12/16
		–	b 2.97 (dd, 8.3, 14.8)	10a	9, 11, 12/16
	11	136.0, C	–		
	12/16	129.6, CH	7.24[d]	13/15	10, 14
	13/15	128.6, CH	7.27[d]	14, 12/16	11
	14	126.9, CH	7.23[d]	13/15	12/16
N-Ac-β-	17	169.2, C	–		
OH-Leu	18	50.3, CH	5.24 (brd, 10.0)	18-NH, 19	17, 19
	18-NH	–	7.55, (d, 10,0)	18	18, 23
	19	77.7, CH	5.10 (brd, 10.0)	18, 20	20, 25
	20	28.8, CH	1.86 (m)	19, 21, 22	
	21	18.9, CH_3	1.01 (d, 6.8)	20	20, 22
	22	18.8, CH_3	0.85 (d, 6.8)	20	20, 21
	23	171.4, C	–		
	24	22.5, CH_3	2.21 (s)		23
N-MeThr(*O*Me)	25	166.5 C	–		
	26	64.4, CH	4.05 (d, 9.6)	27	25
	27	72.3, CH	3.74 (m)	26, 28	26, 28
	28	16.3, CH_3	1.16 (d, 5.8)	27	26, 27
	29	28.7, CH_3	2.68 (s)		26, 31
	30	57.2, CH_3	3.40 (s)		27
β-OH-Leu	31	171.2, C	–		
	32	46.6, CH	5.35 (d, 9.9)	32-NH, 33	31, 33
	32-NH		6.74, (d, 9.9)	32	32, 37
	33	77.0, CH	5.30, (d, 10.0)	32, 34	41
	34	30.5, CH	1.70 (m)	33, 35, 36	35, 36
	35	19.4, CH_3	1.08 (d, 6.7)	34	33, 34, 36
	36	18.3, CH_3	0.82 (d, 6.7)	34	33, 34, 35
N-MeAla	37	169.9, C	–		
	38	56.4, CH	4.70 (q, 6.8)	39	37, 39
	39	14.3, CH_3	1.37 (d, 6.8)	38	37, 38
	40	31.4, CH_3	2.87 (s)		1, 38
N-But-β-	41	170.2, C	–		
OH-Leu	42	56.8, CH	4.55 (brd, 7.8)	42-NH	41
	42-NH	–	7.17 (d, 7.8)	42	42, 47
	43	78.2, CH	3.71 (m)	43-OH, 44	41, 44
	43-OH	–	6.87 (d, 4.2)	43	
	44	30.0, CH	1.96 (m)	43, 45, 46	45, 46
	45	20.5, CH_3	1.15 (6.7)	44	43, 44, 46
	46	18.5, CH_3	0.85 (d, 6.7)	44	43, 44, 45
	47	173.9, C	–		
	48	37.4, CH_2	2.47, m	49	
	49	19.1, CH_2	1.68, m	48, 50	50
	50	13.8, CH_3	0.95 (t, 7.5)	49	48, 49

[**a**]Assignments are based on extensive 1D and 2D NMR measurements (HMBC, HSQC, COSY). ^{13}C-NMR spectra were recorded at 75 MHz. [**b**]Numbers according to Supplementary Figure 24. [**c**] Residues: Ala = alanine, *N*-MeDha = *N*-methyldehydroalanine, D-Pla = D-3-phenyllactic acid, *N*-Ac-β-OH-Leu= *N*-acetylhydroxyleucine, *N*-MeThr(*O*Me) = *N*,*O*-dimethylthreonine, β-OH-Leu = β-hydroxyleucine, *N*-MeAla = *N*-methylalanine, *N*-But-β-OH-Leu = *N*-butyryl-β-hydroxyleucine.[d] overlaying resonances

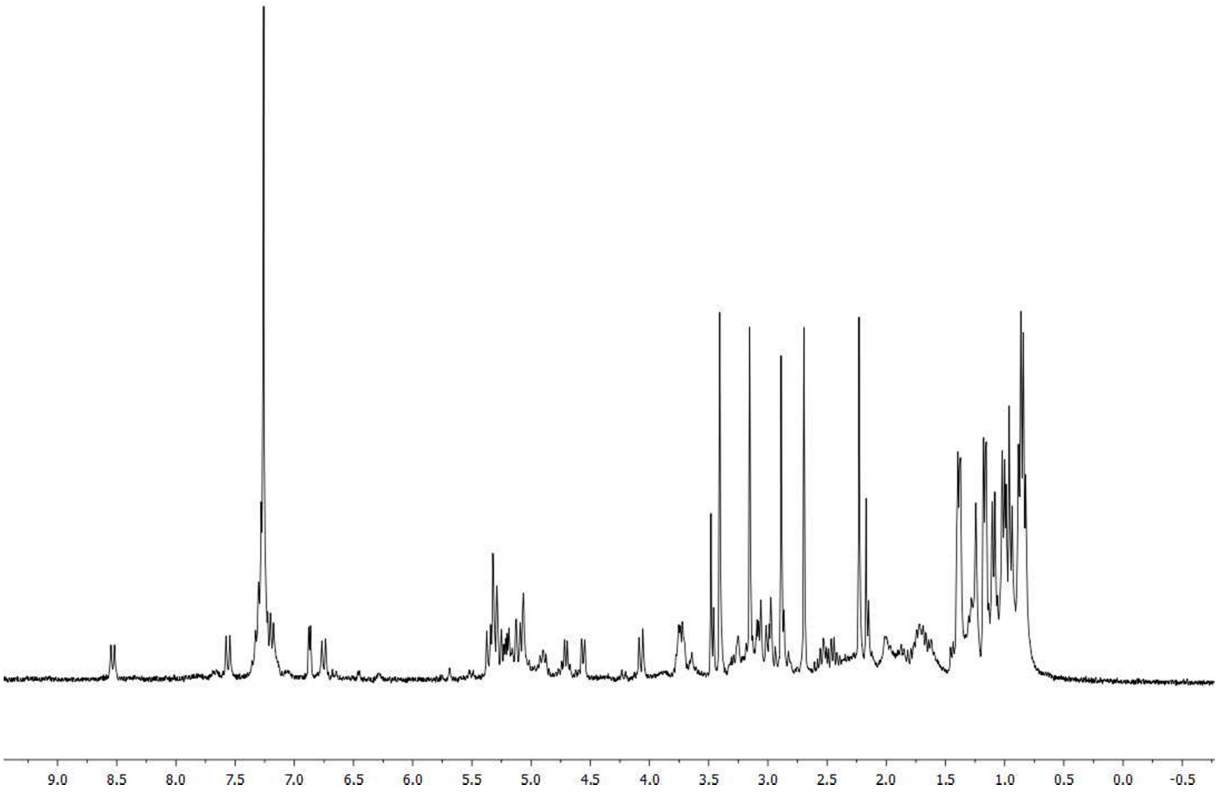

Supplementary Figure 27: ^{1}H NMR spectrum of compound **7** in $CDCl_3$ (300 MHz).

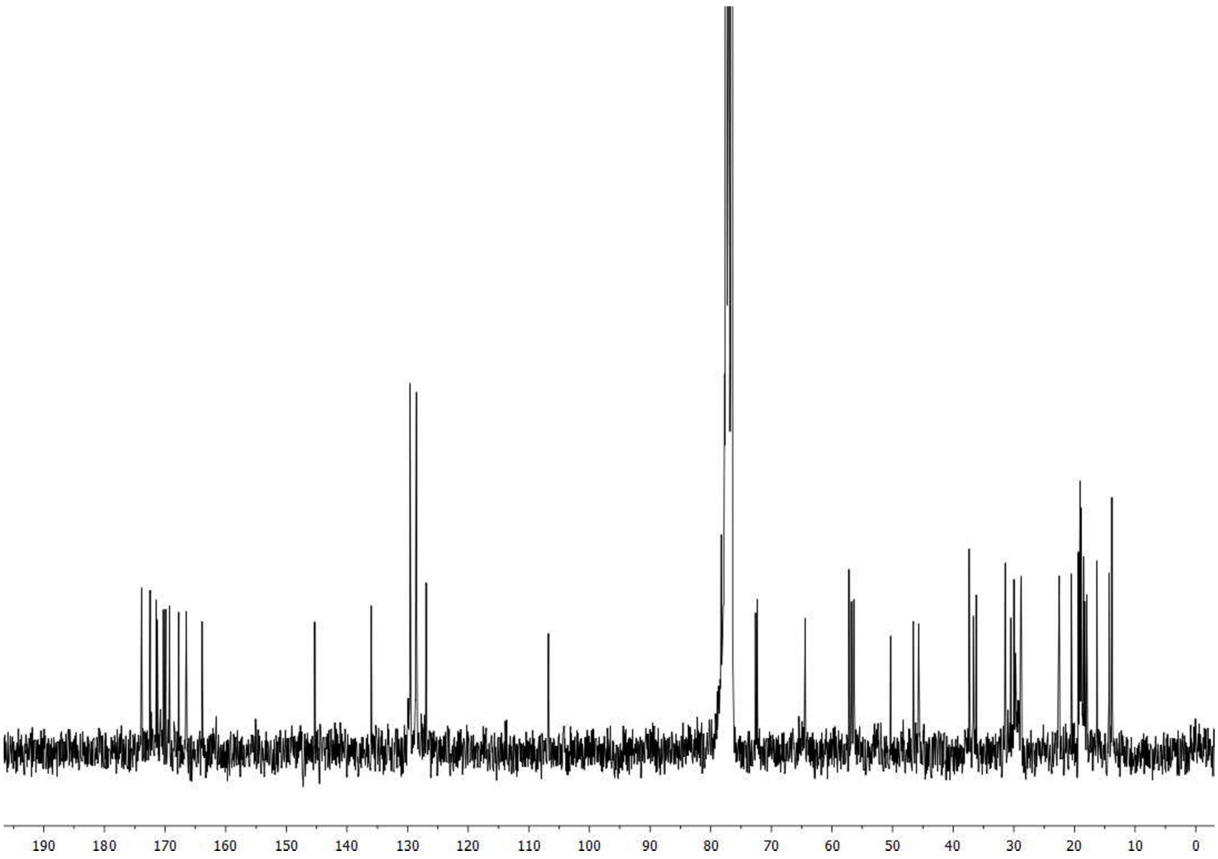

Supplementary Figure 28: ^{13}C NMR spectrum of compound **7** in $CDCl_3$ (75 MHz).

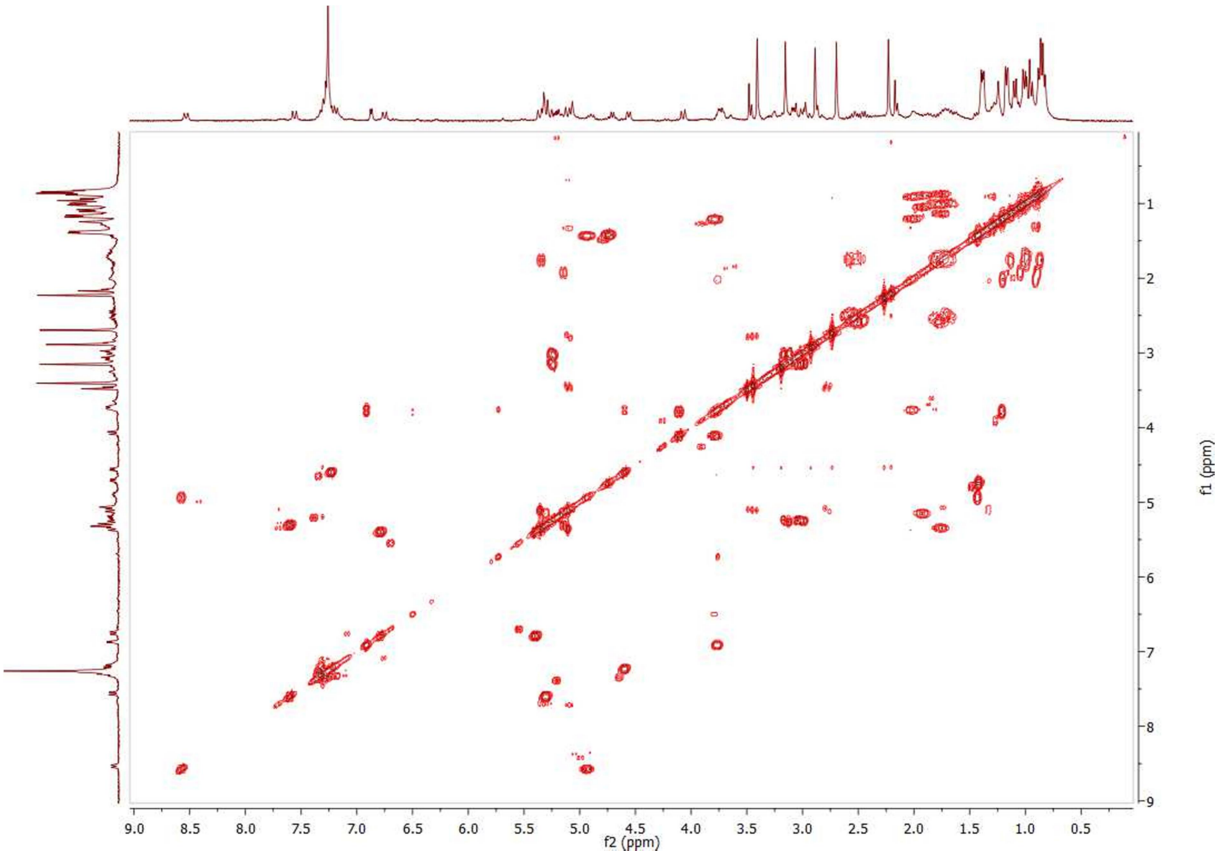

Supplementary Figure 29: ^{1}H-^{1}H COSY NMR spectrum of compound **7** in $CDCl_3$ (300 MHz).

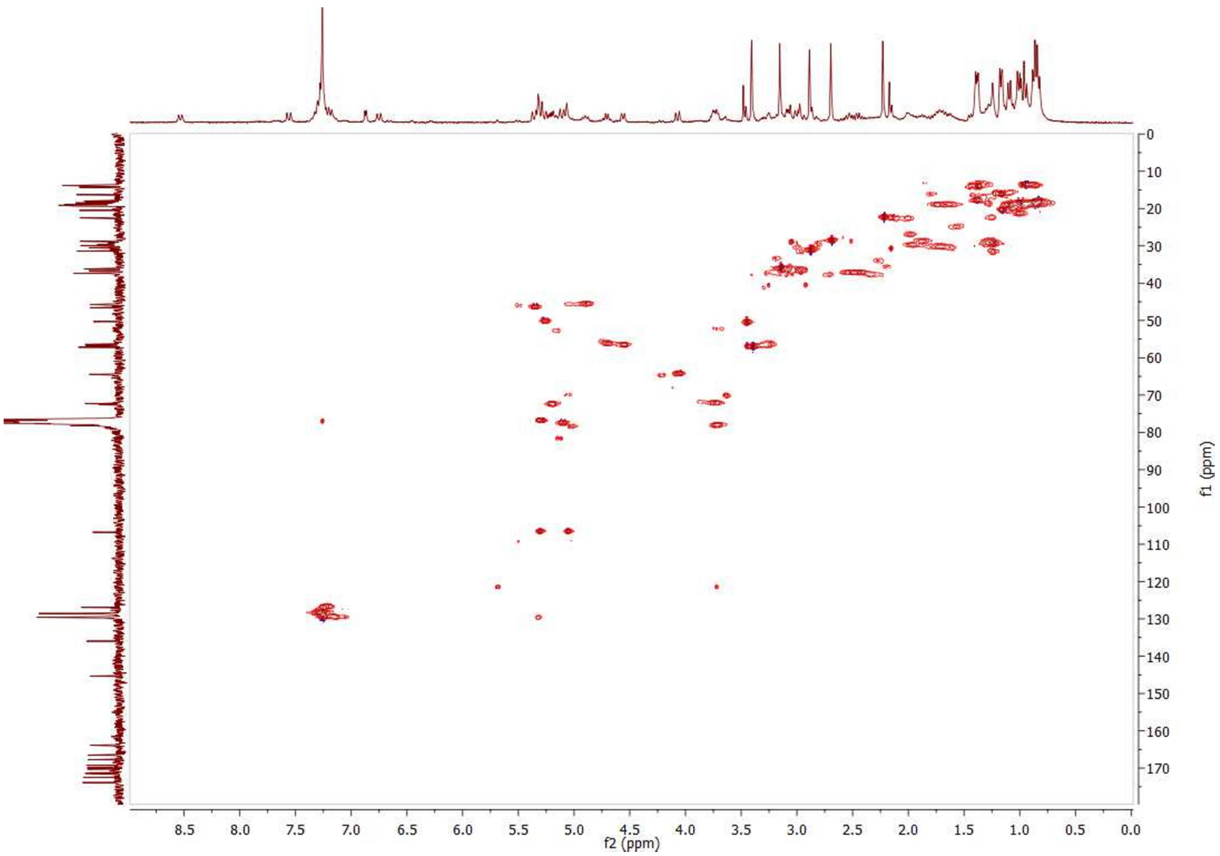

Supplementary Figure 30: ^{1}H-^{13}C HSQC NMR spectrum of compound **7** in $CDCl_3$ (300 MHz).

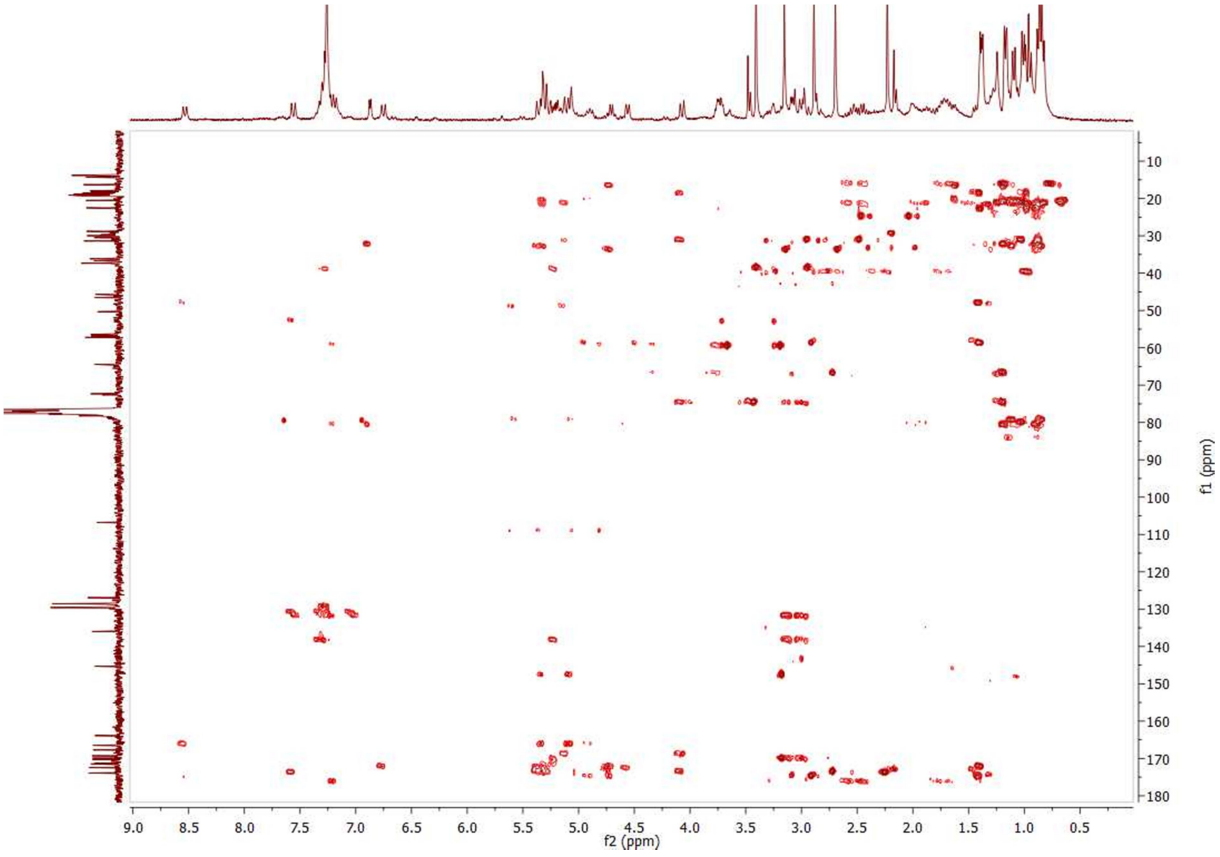

Supplementary Figure 31: ^{1}H-^{13}C HMBC NMR spectrum of compound **7** in $CDCl_3$ (300 MHz).

Gq Inhibition Assays

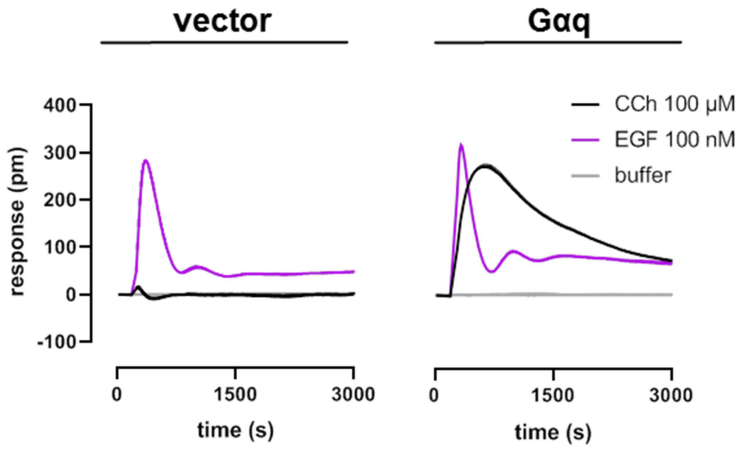

Supplementary Figure 32: CRISPR-Cas9 HEK293 Gαq/Gα11-null cells were unresponsive to carbachol. DMR analysis of whole cell responses evoked by epidermal growth factor (EGF, as viability control) and carbachol (CCh), which activates Gαq-sensitive endogenous muscarinic M3 receptors at the indicated concentrations in CRISPR-Cas9 genome-edited HEK293 cells that lack functional alleles for Gαq and Gα11. Shown are real-time measurements (mean + s.e.m., technical triplicates) representative of three such experiments.

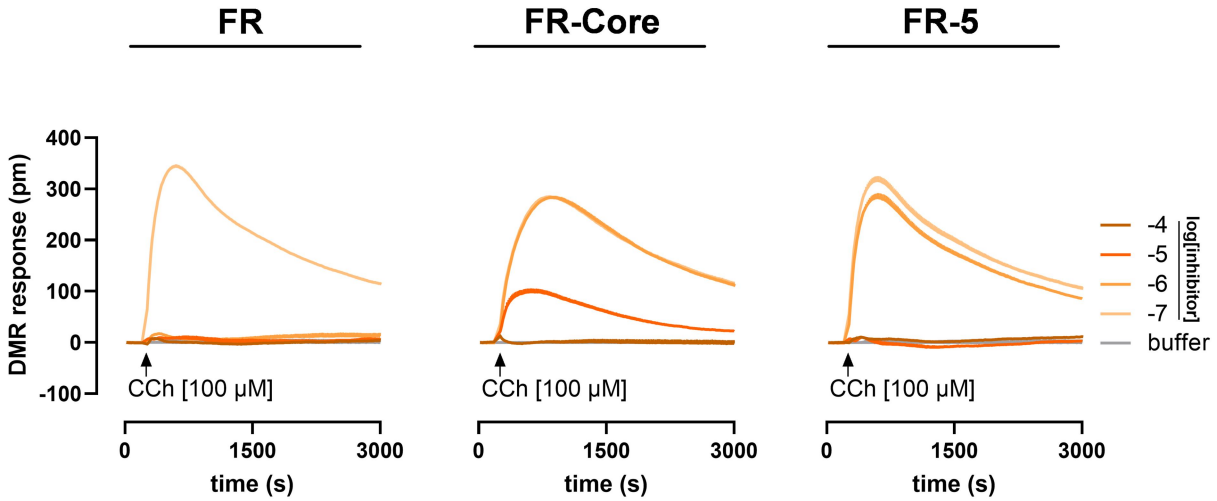

Supplementary Figure 33: Pharmacological characterization of FR-Core and FR-5 on Gαq-mediated signaling. Concentration-dependent inhibition of cell responses induced with carbachol (CCh) [100 µM] by FR, FR-Core and FR-5 in HEK293 Gαq/Gα11-null cells transfected to express wild type Gαq. Data shown are representative real-time recordings (mean + s.e.m., technical triplicates) of at least four independent experiments.

Supplementary Table 6: Quantification of FR, FR-Core and FR-5 inhibitory activities at wild type Gαq in HEK Gαq/Gα11-null cells. IC_{50} values were determined by nonlinear regression on concentration-effect data and represent the mean of 'n' independent biological replicates performed as technical triplicates.

#	pIC_{50}± s.e.m.	IC_{50} [µM]	n
FR (**1**)	6.34±0.03	0.45	11
FR-Core (**2**)	5.13±0.04	7.34	4
FR-5 (**7**)	5.50±0.06	3.18	4

Bioinformatic Analyses on *frs* BGC and FrsA domains

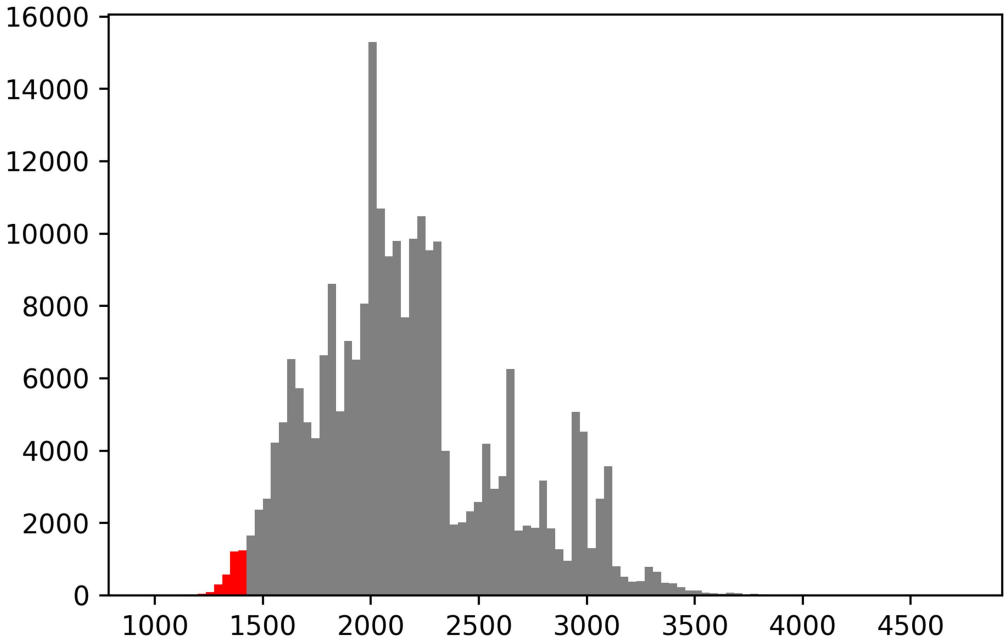

Supplementary Figure 34: Histogram displaying distances of 239,899 BGC relative to *frs* revealed by a BiG-SliCE analysis.[10] X-axis displays distance, y-axis number of BGCs. BGCs marked in red (up to d=1400) were selected for a more detailed BiG-SCAPE analysis.[11]

Supplementary Table 7: Databank accession numbers and source organisms of protein sequences used for phylogenetic analyses of $C_{starter}$ domains. Related to Fig. 5c and Supplementary Fig. 35.

Accession	Organism	Accession	Organism
MT876545	*Chromobacterium vaccinii* MWU205	WP_084480120.1	*Methylosarcina lacus*
MT876545	*Chromobacterium vaccinii* MWU205	WP_078996481.1	*Lysobacter enzymogenes*
KNE75171.1	*Candidatus* Burkholderia crenata	WP_096414584.1	*Lysobacter capsici*
KNE75168.1	*Candidatus* Burkholderia crenata	WP_119629200.1	*Methylocaldum marinum*
WP_162850377.1	*Rhodococcus jostii*	WP_174932260.1	*Burkholderia lata*
WP_007299123.1	*Rhodococcus imtechensis*	WP_120026908.1	*Amycolatopsis panacis*
RZK84214.1	*Rhodococcus sp.*	WP_054261810.1	*Propionispora sp.* 2/2-37
WP_169695704.1	*Rhodococcus opacus*	WP_091794482.1	*Lysobacter sp.* yr284
ELB93997.1	*Rhodococcus wratislaviensis* IFP 2016	WP_040376786.1	*Peribacillus psychrosaccharolyticus*
TMK21117.1	*Alphaproteobacteria bacterium*	WP_138885197.1	*Lysobacter enzymogenes*
TMJ40383.1	*Alphaproteobacteria bacterium*	WP_052756236.1	*Lysobacter capsici*
WP_036714060.1	*Paenibacillus ehimensis*	KJS54231.1	*Streptomyces rubellomurinus subsp. indigoferus*
WP_176165338.1	*Streptomyces sp.* NA00687	WP_166530797.1	*Agaribacter marinus*
WP_106046991.1	*Bacillus atrophaeus*	TQF01515.1	*Kitasatospora sp.* MMS16-CNU292
WP_183596885.1	*Paenibacillus phyllosphaerae*	WP_057921675.1	*Lysobacter capsici*
NQD50526.1	*Bacillus altitudinis*	WP_049786543.1	*Mycetohabitans rhizoxinica*
WP_156746001.1	*Mycobacterium sp.* 1423905.2	CBW76866.1	*Mycetohabitans rhizoxinica* HKI 454
WP_186229549.1	*Burkholderia gladioli*	WP_146064026.1	*Mycetohabitans endofungorum*
OKH99041.1	*Streptomyces sp.* CB02923	WP_174993913.1	*Burkholderia arboris*
WP_157638970.1	*Burkholderia ubonensis*	OPD64588.1	*Lysobacter enzymogenes*

WP_161220653.1	*Streptomyces sp.* SID6137	WP_156123907.1	*Paraburkholderia mimosarum*
WP_155634472.1	*Burkholderia stagnalis*	WP_081052109.1	*Burkholderia cepacia*
REK66978.1	*Brevibacillus sp.*	WP_026869105.1	*Inquilinus limosus*
APD71879.1	*Streptomyces sp.*	WP_143200560.1	*Kitasatospora sp.* CB01950
TDL85614.1	*Vibrio vulnificus*	SFN60854.1	*Actinomadura madurae*
WP_171565203.1	*Brevibacillus sp.* MCWH	WP_051213701.1	*Glomeribacter sp.* 1016415
WP_090670197.1	*Paenibacillus tianmuensis*	WP_067343588.1	*Marinomonas spartinae*
WP_139641914.1	*Streptomyces sedi*	WP_169750257.1	*Streptosporangium amethystogenes*
PBC50623.1	*Rhodococcus sp.* ACS1	WP_092071365.1	*Dendrosporobacter quercicolus*
WP_161218580.1	*Streptomyces sp.* SID6139	WP_045303061.1	*Saccharothrix sp.* ST-888
WP_135342059.1	*Streptomyces palmae*	WP_181556777.1	*Anoxybacillus caldiproteolyticus*
WP_155754571.1	*Burkholderia stagnalis*	WP_034840793.1	*Inquilinus limosus*
WP_161783329.1	*Burkholderia sp.* A1	WP_157441225.1	*Actinoplanes awajinensis*
WP_187438659.1	*Streptomyces sp.* sk2.1	WP_172236540.1	*Bradyrhizobium sp.* LMG 8443
AEA62641.1	*Burkholderia gladioli* BSR3	WP_143956941.1	*Mycobacterium sp.* KBS0706
SEC10944.1	*Rhodococcus koreensis*	WP_165781571.1	*Streptosporangium minutum*
WP_158315302.1	*Bacillus megaterium*	WP_176072366.1	*Paraburkholderia mimosarum*
WP_072274058.1	*Peribacillus simplex*	WP_056114189.1	*Lysobacter sp.* Root690
PAE69549.1	*Bacillus subtilis*	WP_165940603.1	*Burkholderia sp.* SRS-46
WP_120709248.1	*Rhizobium jaguaris*	WP_083780791.1	*Bradyrhizobium sp.* BTAi1
WP_094237092.1	*Tumebacillus algifaecis*	WP_067015022.1	*Marinomonas spartinae*
QAR15116.1	*Streptomyces costaricanus*	PMS18374.1	*Burkholderia dabaoshanensis*
WP_104825816.1	*Rhizobium sp.* NXC24	WP_162791553.1	*Dyella sp.* L4-6
BBA33607.1	*Methylocaldum marinum*	WP_103564835.1	*Actinomadura sp.* RB29
WP_090514810.1	*Paenibacillus sp. cl6col*	RDD80443.1	*Dyella sp.* L4-6
WP_094237092.1	*Tumebacillus algifaecis*	WP_146014032.1	*Burkholderia dabaoshanensis*
WP_098680385.1	*Bacillus altitudinis*	WP_132240709.1	*Micromonospora sp.* CNZ303
WP_081114287.1	*Bacillus stratosphericus*	WP_091621489.1	*Micromonospora peucetia*
WP_068017976.1	*Rhodoplanes sp.* Z2-YC6860	WP_093292387.1	*Thermoactinomyces sp.* DSM 45892
WP_181799076.1	*Kitasatospora sp.* MMS16-CNU292	WP_184260366.1	*Granulicella mallensis*
WP_061420802.1	*Bacillus pumilus*	WP_067109092.1	*Mycobacterium sp.* 852002-51057_SCH5723018
WP_125058029.1	*Streptomyces rimosus*	WP_110573648.1	*Marinomonas alcarazii*
WP_128788709.1	*Streptomyces sp. endophyte*_N2	WP_033674841.1	*Bacillus gaemokensis*
PYS27789.1	*Acidobacteria bacterium*	WP_172427363.1	*Streptomyces griseofuscus*
WP_048411362.1	*Chromobacterium sp.* LK1	WP_157419571.1	*Actinomadura kijaniata*
WP_099396555.1	*Iodobacter sp.* BJB302	WP_186145144.1	*Burkholderia gladioli*
AXE32757.1	*Chromobacterium sp.* IIBBL 112-1	WP_007952768.1	*Pelosinus fermentans*
WP_082113610.1	*Chromobacterium vaccinii*	WP_136371369.1	*Cohnella sp.* CC-MHH1044
WP_122983744.1	*Chromobacterium subtsugae*	WP_076788272.1	*Burkholderia sp.* b13
KZE85028.1	*Chromobacterium sp.* F49	WP_146012759.1	*Trinickia caryophylli*
SUX53575.1	*Chromobacterium vaccinii*	WP_146064107.1	*Mycetohabitans endofungorum*
OVE47519.1	*Chromobacterium violaceum*	WP_142401196.1	*Mycobacterium marinum*
WP_081545507.1	*Chromobacterium haemolyticum*	WP_067015692.1	*Mycobacterium sp.* 1081908.1
WP_118266927.1	*Chromobacterium rhizoryzae*	WP_052407967.1	*Allokutzneria albata*
WP_106076243.1	*Chromobacterium amazonense*	MPZ86334.1	*Actinophytocola sp.*
WP_107800191.1	*Chromobacterium sp. Panama*	WP_141996174.1	*Amycolatopsis cihanbeyliensis*
WP_156746001.1	*Mycobacterium sp.* 1423905.2	KAK48742.1	*Caballeronia jiangsuensis*
WP_175879783.1	*Mycobacterium sp.* IS-2888	WP_099661199.1	*Sporosarcina sp.* P29
WP_172880913.1	*Bacillus safensis*	WP_066488029.1	*Burkholderia sp.* BDU8
WP_097231083.1	*Streptomyces zhaozhouensis*	WP_073604292.1	*Vibrio aerogenes*
WP_053416733.1	*Viridibacillus arvi*	SAL02479.1	*Caballeronia arationis*
WP_143665067.1	*Streptomyces cacaoi*	NVK71858.1	*Oceanospirillaceae bacterium*
WP_123647243.1	*Lysobacter enzymogenes*	WP_061162849.1	*Caballeronia temeraria*
WP_035299007.1	*Brevibacillus thermoruber*	SLC21331.1	*Mycobacteroides abscessus subsp. massiliense*
WP_076794250.1	*Burkholderia sp.* b14		

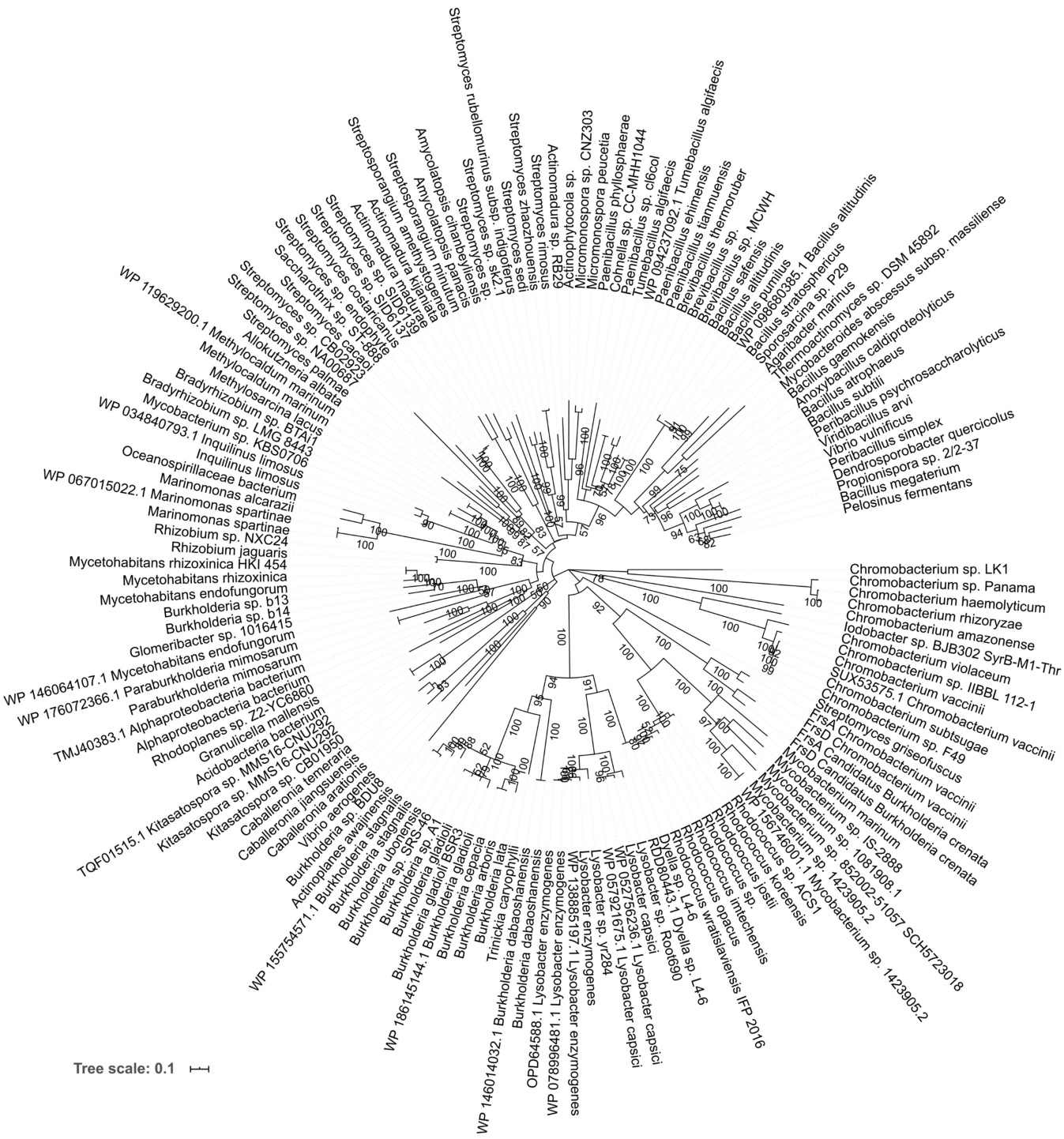

Supplementary Figure 35: Phylogenetic tree of NRPS $C_{Starter}$ domains. The scale bar represents 20 substitutions per 100 amino acids. Related to Figure 5c. For experimental details, see Methods Section and Supplementary Table 8.

```
TE_FrsA            1 HPLFCIHPEGGLGWSYIGLALHLDHEQPIYTLQARGLDGMSELAPSIPDM     50
                     .|||||||.|.|.|:|:.|..:||.|||||.|||||:||.||.|.||..|
TE_FrsG            1 PPLFCIHPGGCLSWTYVSLVRYLDAEQPIYGLQARGIDGQSEPASSIEAM     50

TE_FrsA           51 AADYIEQIRSIQPNGPYHLLGWSLGGVIAQEVAVQLERVGEKTALLAILD    100
                     ||||:.|||.|||:|||:|||||||||.:|||.:|.|||.:.::..||.:||
TE_FrsG           51 AADYVAQIRGIQPHGPYYLLGWSLGGNLAQAMASQLESMDQEVGLLFLLD    100

TE_FrsA          101 TFPIEILHEAMFGKQACAYDLFARVVQEMYLMPIEEARLKSMYLIGLNHM    150
                     :.| ..:|:   ..:...|.||.:..:..:..:.|.:::::::.:...|:
TE_FrsG          101 SGP-SPMHK---DDEMIEYPLFTKEFKNTFKFHVSETKMQAIFEVTKRHV    146

TE_FrsA          151 KITAAFSSSHYGGDLLLFRSLIPYAEDALMPEADTWQPYLSGQLEVHDIE    200
                     ::....:....|..||||:.:||.|...:.....|..|:.|.:|||::.
TE_FrsG          147 ELIRQSTTPVSQGPALLFRATVPYDESTPLLPPHAWNEYVKGDIEVHEVH    196

TE_FrsA          201 CTHMDMMQRDVLKIIGPVLESKL    223
                     |.|..|.:.:.:::.:|||:|.||
TE_FrsG          197 CQHAQMNRIEFMEQMGPVIERKL    219

                              Length: 223
                    # Identity:      93/223 (41.7%)
                    # Similarity:   139/223 (62.3%)
                    # Gaps:           4/223 (1.8%)
                    # Score: 482.0
```

Supplementary Figure 36: Emboss Needle Alignment of $FrsA_{TE}$ and $FrsG_{TE}$ from *C. vaccinii*. Residues in the active site, which are responsible for hydrolysis, are marked in yellow.

Supplementary Table 8: Names, databank accession numbers, source organisms of protein sequences used for phylogenetic analyses of TE domains. Related to Fig. 5d.

Name	Accession	Organism
BcFrsA-TE	KNE75171.1	*"Candidatus* Burkholderia crenata"
BcFrsG-TE	KNE75165.1	*"Candidatus* Burkholderia crenata"
cvFrsA-TE	MT876545	*Chromobacterium vaccinii* MWU205
cvFrsG-TE	MT876545	*Chromobacterium vaccinii* MWU205
DhbF - TE	WP_144530663.1	*Bacillus subtilis* ATCC 21332
EntF - TE	AYG20286.1	*Escherichia coli str.* K-12 *substr.* MG1655
ERYA3_TE	Q03133	*Saccharopolyspora erythraea*
FtdB - TE	ADJ54381.1	*Streptomyces sp.* SPB78
HbnA	ALV82446.1	*Streptomyces variabili*
HSAF - TE	ABL86391.1	*Lysobacter enzymogenes*
IkaA - TE	AJD77023.1	*Streptomyces sp.* ZJ306
KirHI	AGS67165.1	*Streptomyces collinus* Tu 365
KSE_70420	BAJ32800	*Kitasatospora setae* KM-6054
LipX2	ABB05100	*Streptomyces aureofaciens*
LybB - TE1	AEH59100.1	*Lysobacter sp.* ATCC 53042
LybB - TE2	AEH59100.1	*Lysobacter sp.* ATCC 53042
MassC - TE1	EIK63041.1	*Pseudomonas fluorescens* SS101
MassC - TE2	EIK63041.1	*Pseudomonas fluorescens* SS101
NocB - TE	AAT09805.1	*Nocardia uniformis subsp. tsuyamanensis*
ObiF - TE	KX134687.1	*Pseudomonas fluorescens* ATCC 39502
Pys-Pent - TE	WP_011533552	*Pseudomonas entomophila*
Pys-Pflu -TE	WP_064118616	*Pseudomonas fluorescens* HKI 0770
RomH	WP_078586793.1	*Streptomyces rimosus* NRRL B-2659
RomI	WP_004571777.1	*Streptomyces rimosus* NRRL B-2659
SGR814 - TE	AGK81502	*Streptomyces fulvissimus* DSM 40593
SlgL	CBA11558	*Streptomyces lydicus*
Sln6 - TE	DAB41476.1	*Streptomyces sp.* CNB-091
Sln9 - TE	DAB41479.1	*Streptomyces sp.* CNB-091
SrfA-C - TE	2VSQ	*Bacillus subtilis* ATCC 21332
SSHG - TE	EFE85271.1	*Streptomyces albus* J1074
SwrW - TE	I7GF64	*Serratia marcescens*

TaaE - TE1	CCJ67640.1	*Pseudomonas costantinii* DSM 16734
TaaE - TE2	CCJ67640.1	*Pseudomonas costantinii*
TrdC	ADY38535.1	*Streptomyces sp.* SCSIO 1666
TycC - TE	AAC45930.1	*Brevibacillus brevis*
ViscC - TE1	CAY48789.1	*Pseudomonas fluorescens* SBW25
ViscC - TE2	CAY48789.1	*Pseudomonas fluorescens* SBW25
WlipC - TE1	AFJ23826.1	*Pseudomonas putida*
WlipC - TE2	AFJ23826.1	*Pseudomonas putida*

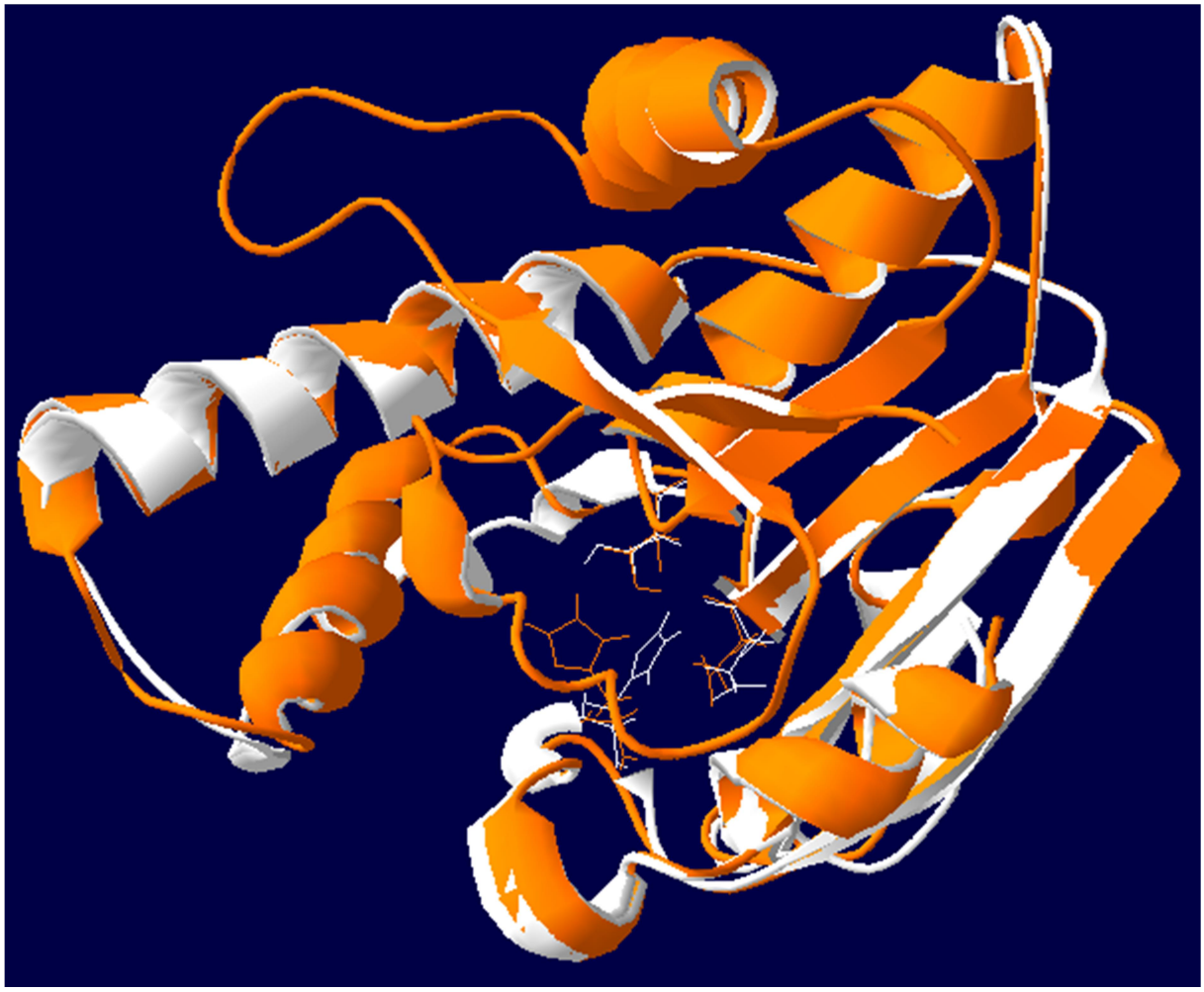

Supplementary Figure 37: Alignment of the structural models of $FrsA_{TE}$ (orange) and $FrsG_{TE}$ (white) from *C. vaccinii*. The amino acids of the active site are displayed in red (FrsA) and blue (FrsG).

Discussion: $FrsA_{TE}$ acceptor substrate specificity

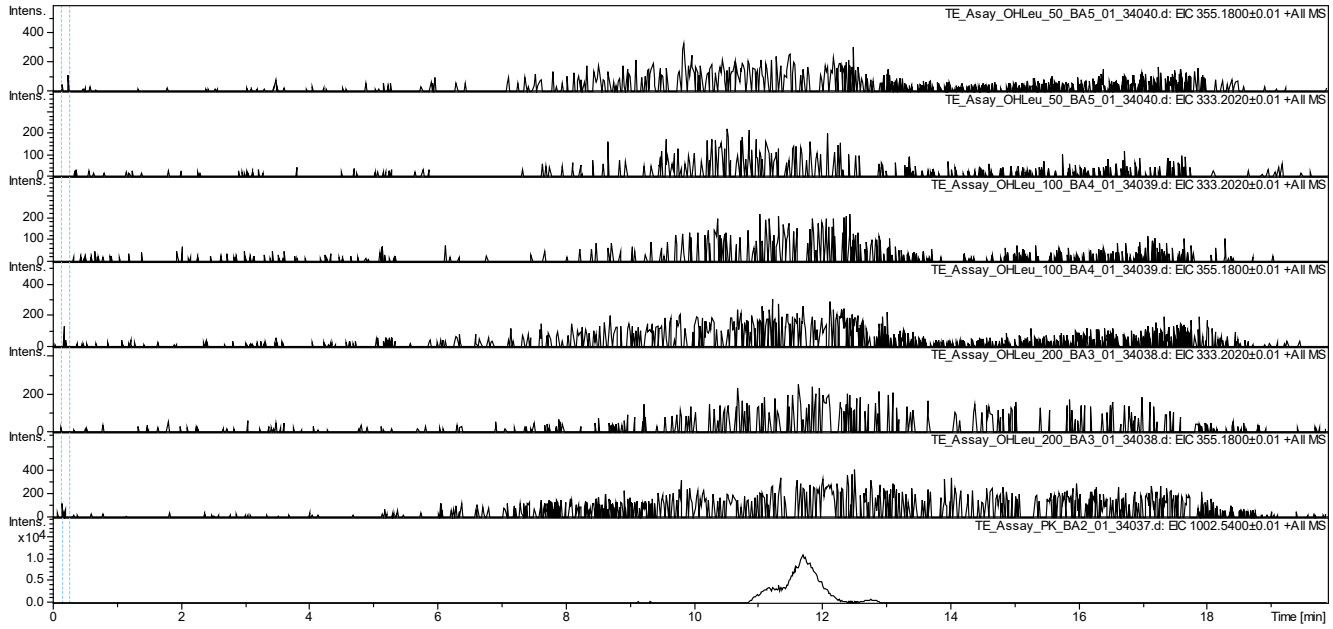

Supplementary Figure 38: EICs of HPLC-MS experiments of transesterification assays with the added minimal substrate Hle in varying concentrations (50 µM, 100 µM, 200 µM), instead of **2**. EIC for the proton adduct (*m/z*: 333.202) and the sodium adduct (*m/z*: 355.180) of the anticipated product Hle-N-Pp-Hle ester were generated. Also, the data was analyzed for formation of dimer and trimer esters. No product formation could be observed. FrsA TE was reconstituted in active conformation in this assay, as can be seen from the positive control experiment in the bottom chromatogram (formation of **1** after addition of **2**).

Supplementary References

[1] Carlier, A. et al. The genome analysis of Candidatus Burkholderia crenata reveals that secondary metabolism may be a key function of the Ardisia crenata leaf nodule symbiosis. *Environ. Microbiol.* **18,** 2507–2522 (2016).

[2] Madeira, F. et al., The EMBL-EBI search and sequence analysis tools APIs in 2019. *Nucleic Acids Res.* **47,** W636–W641 (2019).

[3] Hoang, T. T., Karkhoff-Schweizer, R. R., Kutchma, A. J., Schweizer, H. P. A broad-host-range Flp-FRT recombination system for site-specific excision of chromosomally-located DNA sequences: application for isolation of unmarked Pseudomonas aeruginosa mutants. *Gene* **212,** 77–86 (1998).

[4] Norrander, J., Kempe, T., Messing, J. Construction of improved M13 vectors using oligodeoxynucleotide-directed mutagenesis. *Gene* **26,** 101–106 (1983).

[5] Gibson, D. G., Young, L., Chuang, R. Y., Venter, J. C., Hutchison 3rd, C. A., Smith, H. O. Enzymatic assembly of DNA molecules up to several hundred kilobases. *Nat. Methods* **6,** 343–345 (2009).

[6] Lynch, M. D., Gill, R. T. Broad host range vectors for stable genomic library construction. *Biotechnol. Bioeng.* **94,** 151–158 (2006).

[7] Wang, C., Wesener, S. R., Zhang, H. Cheng, Y.-Q. An FAD-dependent pyridine nucleotide-disulfide oxidoreductase is involved in disulfide bond formation in FK228 anticancer depsipeptide. *Chem. Biol*. **16,** 585-593 (2009).

[8] Broetto, L., Cecagno, R., Sant'Anna, F. H., Weber, S., Schrank, I. S. Stable transformation of Chromobacterium violaceum with a broad-host-range plasmid. *Appl. Microbiol. Biotechnol.* **71,** 450–454 (2006).

[9] Reher, R. et al. Applying molecular networking for the detection of natural sources and analogues of the selective Gq Protein inhibitor FR900359. *J Nat. Prod.* **81,** 1628–1635 (2018).

[10] Kautsar, S.A., van der Hooft, J.J.J., de Ridder, D., Medema, M.H. BiG-SLiCE: A highly scalable tool maps the diversity of 1.2 million biosynthetic gene clusters. *bioRxiv* (2020).

[11] Navarro-Muñoz, J. C., et al. A computational framework to explore large-scale biosynthetic diversity. *Nat. Chem. Biol.* **16,** 60-68 (2020).